ARTICLE

LIS1 regulates cargo-adapter–mediated activation of dynein by overcoming its autoinhibition in vivo

Rongde Qiu, Jun Zhang , and Xin Xiang

Deficiency of the LIS1 protein causes lissencephaly, a brain developmental disorder. Although LIS1 binds the microtubule motor cytoplasmic dynein and has been linked to dynein function in many experimental systems, its mechanism of action remains unclear. Here, we revealed its function in cargo-adapter–mediated dynein activation in the model organism *Aspergillus nidulans*. Specifically, we found that overexpressed cargo adapter HookA (Hook in *A. nidulans*) missing its cargo-binding domain (ΔC-HookA) causes dynein and its regulator dynactin to relocate from the microtubule plus ends to the minus ends, and this relocation requires LIS1 and its binding protein, NudE. Astonishingly, the requirement for LIS1 or NudE can be bypassed to a significant extent by mutations that prohibit dynein from forming an autoinhibited conformation in which the motor domains of the dynein dimer are held close together. Our results suggest a novel mechanism of LIS1 action that promotes the switch of dynein from the autoinhibited state to an open state to facilitate dynein activation.

Introduction

Cytoplasmic dynein-1 (called dynein hereafter) is a microtubule (MT) motor that transports a variety of cargos in eukaryotic cells, and defects in dynein-mediated transport are linked to devastating neurodegenerative diseases and brain developmental disorders (Maday et al., 2014; Jaarsma and Hoogenraad, 2015; Bertipaglia et al., 2018). The dynein–cargo interaction requires the multicomponent dynactin complex as well as specific cargo adapters (Schroer, 2004; Akhmanova and Hammer, 2010; Fu and Holzbaur, 2014; Reck-Peterson et al., 2018; Olenick and Holzbaur, 2019). Importantly, dynactin and cargo adapters also activate the motility of cytoplasmic dynein in vitro (McKenney et al., 2014; Schlager et al., 2014; Reck-Peterson et al., 2018; Olenick and Holzbaur, 2019). The mechanism underlying this activation was suggested by a recent cryo-EM analysis (Zhang et al., 2017a). Specifically, the two motor domains of the dynein heavy chain (HC) dimer are held together in an inactive "phi" conformation (Torisawa et al., 2014; Zhang et al., 2017a), which is in equilibrium with an "open" conformation in which the two domains are separated. While dynein in the "open" conformation is still not configured properly to move directionally along MTs by itself, its binding to dynactin and cargo adapter causes the HC dimer to become parallel for directional movement along MTs (Zhang et al., 2017a). Moreover, some cargo adapters facilitate the recruitment of a second dynein dimer to dynactin (Grotjahn et al., 2018; Urnavicius et al., 2018), further enhancing dynein force and speed (Urnavicius et al., 2018). While these

are important steps toward understanding dynein regulatory mechanisms, the cargo-adapter-mediated dynein activation has never been analyzed in vivo, and it is especially unclear whether this process is regulated by other proteins in vivo.

Two of the most well-known yet enigmatic dynein regulators are LIS1 and its binding partner, NudE (Kardon and Vale, 2009; Vallee et al., 2012; Reck-Peterson et al., 2018; Olenick and Holzbaur, 2019). LIS1 is encoded by the *lis1* gene, whose deficiency causes type I lissencephaly, a human brain developmental disorder (Reiner et al., 1993). Fungal genetic studies first linked LIS1 to dynein function (Xiang et al., 1995a; Geiser et al., 1997; Willins et al., 1997). In the filamentous fungus *Aspergillus nidulans*, the LIS1 homologue NudF is critical for dynein-mediated nuclear distribution (Xiang et al., 1995a). *A. nidulans* genetics also led to the identification of NudE, a NudF/LIS1-binding protein (Efimov and Morris, 2000; Feng et al., 2000; Niethammer et al., 2000; Sasaki et al., 2000), whose homologues participate in dynein function in various systems (Minke et al., 1999; Liang et al., 2004, 2007; Li et al., 2005a; Stehman et al., 2007; Yamada et al., 2008; Kardon and Vale, 2009; Ma et al., 2009; Zhang et al., 2009; Lam et al., 2010; Pandey and Smith, 2011; Wang and Zheng, 2011; Zyłkiewicz et al., 2011; Vallee et al., 2012; Raaijmakers et al., 2013; Wang et al., 2013; Klinman and Holzbaur, 2015; Kuijpers et al., 2016; Simões et al., 2018; Olenick and Holzbaur, 2019). The mechanism by which these two proteins regulate dynein remains unclear. The dynein

Department of Biochemistry and Molecular Biology, the Uniformed Services University F. Edward Hébert School of Medicine, Bethesda, MD.

Correspondence to Xin Xiang: xin.xiang@usuhs.edu.

HC contains six AAA domains in its motor ring (King, 2000; Asai and Koonce, 2001), and LIS1 binds AAA3/AAA4 and the stalk leading to the MT-binding domain (Huang et al., 2012; Toropova et al., 2014; DeSantis et al., 2017). Intriguingly, purified LIS1 inhibits dynein motility in vitro (Yamada et al., 2008; McKenney et al., 2010; Huang et al., 2012), unless ATP hydrolysis at AAA3 is blocked (DeSantis et al., 2017). NudE/Nudel (also called NDEL1) relieves the inhibitory effect of LIS1 (Yamada et al., 2008; Torisawa et al., 2011), and the NudE–LIS1 complex enhances dynein force production (McKenney et al., 2010; Reddy et al., 2016). Moreover, dynactin partially relieves the inhibition of LIS1 on dynein motility (Wang et al., 2013), and when both dynactin and cargo adapter are present, LIS1 no longer inhibits but mildly enhances the dynein movement (Baumbach et al., 2017; Gutierrez et al., 2017; Jha et al., 2017). However, the exact molecular mechanism of LIS1 action on dynein regulation is not known (Reck-Peterson et al., 2018; Olenick and Holzbaur, 2019).

We have been using the fungal model organism *A. nidulans* to investigate dynein regulation in vivo. Unlike budding yeast, where dynein is required almost exclusively for nuclear migration/spindle orientation (Eshel et al., 1993; Li et al., 1993), dynein, dynactin, and LIS1 in filamentous fungi are required not only for nuclear distribution (Plamann et al., 1994; Xiang et al., 1994, 1995a) but also for transporting a variety of other cargos, including early endosomes and their hitchhiking partners (Wedlich-Söldner et al., 2002; Lenz et al., 2006; Abenza et al., 2009; Zekert and Fischer, 2009; Baumann et al., 2012; Bielska et al., 2014a; Higuchi et al., 2014; Egan et al., 2015; Guimaraes et al., 2015; Pohlmann et al., 2015; Salogiannis et al., 2016; Peñalva et al., 2017; Otamendi et al., 2019). In filamentous fungi and budding yeast, dynein, dynactin, and LIS1–NudE all accumulate at the MT plus ends (Han et al., 2001; Efimov, 2003; Lee et al., 2003; Sheeman et al., 2003; Zhang et al., 2003; Li et al., 2005a; Lenz et al., 2006; Moore et al., 2008; Callejas-Negrete et al., 2015). The MT plus-end accumulation of dynein is important for spindle-orientation/nuclear migration and for early endosome transport (Lee et al., 2003; Sheeman et al., 2003; Lenz et al., 2006; Omer et al., 2018; Xiang, 2018). In *A. nidulans* and *Ustilago maydis,* plus end dynein accumulation depends on dynactin and kinesin-1, but not NudF/LIS1 (Zhang et al., 2003, 2010; Lenz et al., 2006; Egan et al., 2012; Yao et al., 2012). This differs from the situation in budding yeast, where LIS1 is critical for dynein's plus-end accumulation, and in mammalian cells, where both LIS1 and dynactin are critical (Lee et al., 2003; Sheeman et al., 2003; Splinter et al., 2012). Recently, the interaction between fungal dynein and early endosome has been found to be mediated by dynactin as well as the Fhip–Hook–Fts complex (Walenta et al., 2001; Xu et al., 2008; Zhang et al., 2011, 2014; Bielska et al., 2014b). Within the Fhip–Hook–Fts complex, Hook (HookA in *A. nidulans* and Hok1 in *U. maydis*) interacts with dynein–dynactin and Fhip interacts with early endosome (Bielska et al., 2014b; Yao et al., 2014; Zhang et al., 2014; Guo et al., 2016; Schroeder and Vale, 2016). The function of dynactin and the Hook complex in early endosome transport is evolutionarily conserved (although multiple Hook proteins in mammalian cells participate in even more functions of dynein; Yeh et al., 2012; Guo et al., 2016; Dwivedi et al., 2019; Olenick et al., 2019), and importantly, mammalian Hook proteins activate dynein in vitro (McKenney et al., 2014; Olenick et al., 2016; Schroeder and Vale, 2016).

Here, we developed a new assay to examine HookA-mediated dynein activation in *A. nidulans* and revealed the role of LIS1 in this context. Specifically, we overexpressed HookA lacking the C-terminal early endosome-binding site (ΔC-HookA), which binds dynein–dynactin, but not early endosome (Zhang et al., 2014). In contrast to the MT plus-end accumulation of dynein–dynactin in wild-type cells, ΔC-HookA overexpression shifts the accumulation to the MT minus ends. LIS1 and its binding protein, NudE, are both required for this cargo-adapter–mediated dynein relocation in vivo. Interestingly, dynein mutations that open up the autoinhibited phi conformation of dynein allow the requirement of LIS1 or NudE to be bypassed to a significant extent in vivo. We suggest that the function of LIS1 is linked to a key step of dynein activation: shifting from the autoinhibited phi conformation to an open conformation that allows dynein to be fully activated.

Results

Dynein and dynactin are relocated from the MT plus ends to the minus ends upon overexpression of ΔC-HookA

To examine cargo-adapter–mediated dynein activation in vivo, we sought to create *A. nidulans* cells where dynein and dynactin are occupied by cytosolic cargo adapters. To do that, we replaced the wild-type *hookA* allele with the *gpdA-ΔC-hookA*-S allele so that ΔC-HookA (missing its cargo-binding site) is overexpressed under the constitutive *gpdA* promoter (Fig. 1, A and B; and Fig. S1, A and B; Pantazopoulou and Peñalva, 2009; Zhang et al., 2011). Overexpression of ΔC-HookA did not inhibit colony growth significantly (Fig. 1 C) but caused a partial nuclear-distribution defect (Fig. S1, C and D), possibly due to a loss of dynein's MT plus-end accumulation (see below; Xiang, 2018). In wild-type strains, GFP-labeled dynein and dynactin (p150 subunit) formed comet-like structures near the hyphal tip, representing their MT plus-end accumulation (Han et al., 2001; Zhang et al., 2003; Fig. 1, D–F). Upon overexpression of ΔC-HookA, the plus-end comets of dynein or dynactin disappeared from almost all hyphal tips (Fig. 1, D–F), although signals along MT-like tracks were seen in some hyphae (Figs. 1 D and S2 A). This was not caused by a defect in MT organization, because mCherry-labeled ClipA/Clip170 (Zeng et al., 2014) formed plus-end comets in the same cells (Fig. 1 D). A dominant feature in these cells is the accumulation of dynein and dynactin at septa, which are structures known to contain active MT-organizing centers (MTOCs; Konzack et al., 2005; Xiong and Oakley, 2009; Zekert et al., 2010; Zhang et al., 2017b; Fig. 1, E and F). In some of these cells, movement of GFP-dynein toward a septum can be observed (Fig. S2 A and Video 1). Dynein at septa was found in wild-type cells (Liu et al., 2003), but the signals were much less obvious compared with the strong accumulation upon ΔC-HookA overexpression (Fig. 1 E). Besides septal MTOCs, the nuclear envelope–associated spindle-pole body (SPB) represents the earliest-discovered MTOC (Oakley et al., 1990). Previously,
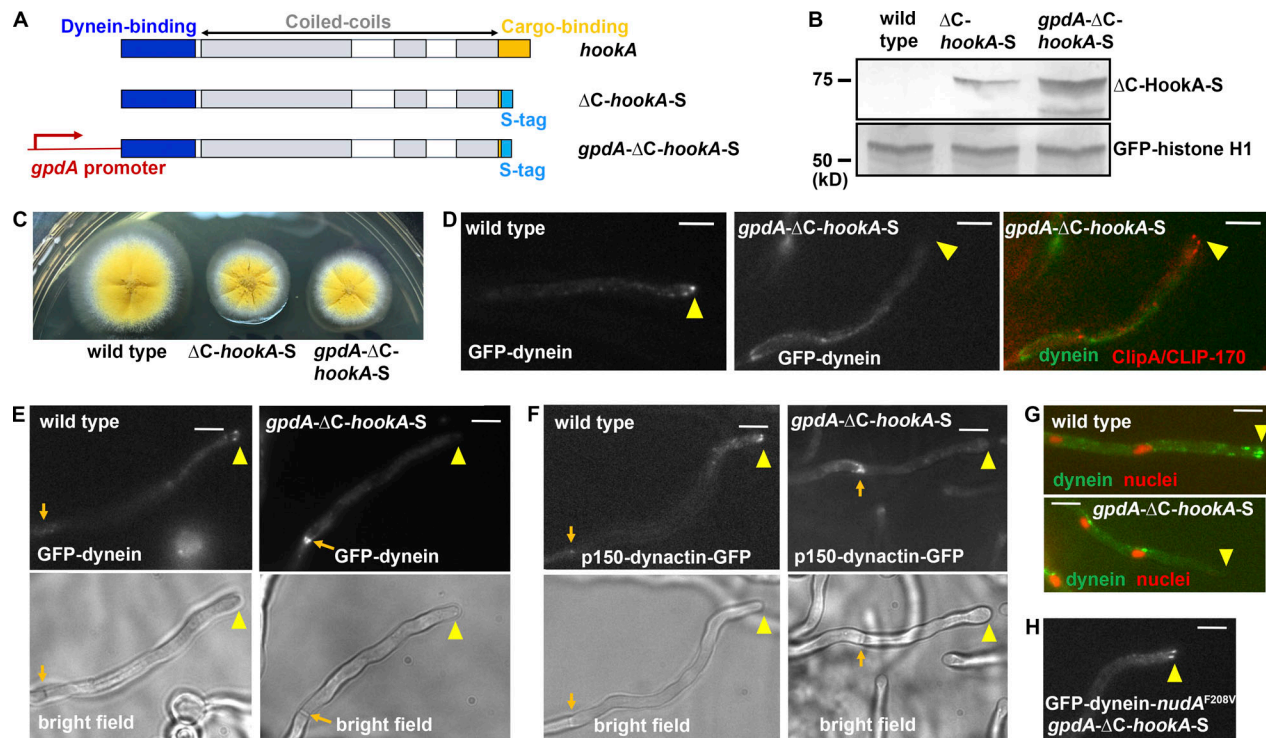
Figure 1. **Overexpression of ΔC-HookA by the *gpdA* promoter drives dynein–dynactin relocation from the MT plus ends to the minus ends. (A)** A diagram showing the wild-type *hookA* allele, the ΔC-*hookA*-S allele, and the *gpdA*-ΔC-*hookA*-S allele. **(B)** Western blots showing the ΔC-HookA-S protein being overexpressed by the *gpdA* promoter. GFP-histone H1 was used as a loading control. **(C)** Colony phenotype of a *gpdA*-ΔC-*hookA*-S strain in comparison to that of a wild-type control and a ΔC-*hookA*-S strain. **(D)** Images of GFP-dynein in wild-type and *gpdA*-ΔC-*hookA*-S strains. Plus-end dynein comets near the hyphal tip (arrowheads) are present in wild-type, but not in a *gpdA*-ΔC-*hookA*-S hypha, although the plus-end comets of mCherry-ClipA/CLIP-170 are present in the same *gpdA*-ΔC-*hookA*-S hypha. Brightness is increased by 30% for all three images. **(E)** Accumulation of GFP-dynein as plus-end comets in a wild-type control and on a septum (arrows) in a *gpdA*-ΔC-*hookA*-S strain. Bright-field images are shown below to indicate hyphal shape and position of the septum. **(F)** Accumulation of p150-dynactin-GFP as plus-end comets in a wild-type control and on a septum in a *gpdA*-ΔC-*hookA*-S strain. **(G)** The localization of GFP-dynein on nuclei labeled with NLS-DsRed in the *gpdA*-ΔC-*hookA*-S strain. A wild-type control is presented. Brightness is increased by 50% for both images. **(H)** Plus-end dynein comets in the *nudA*F[208V], *gpdA*-ΔC-*hookA*-S strain. Bars, 5 µm.
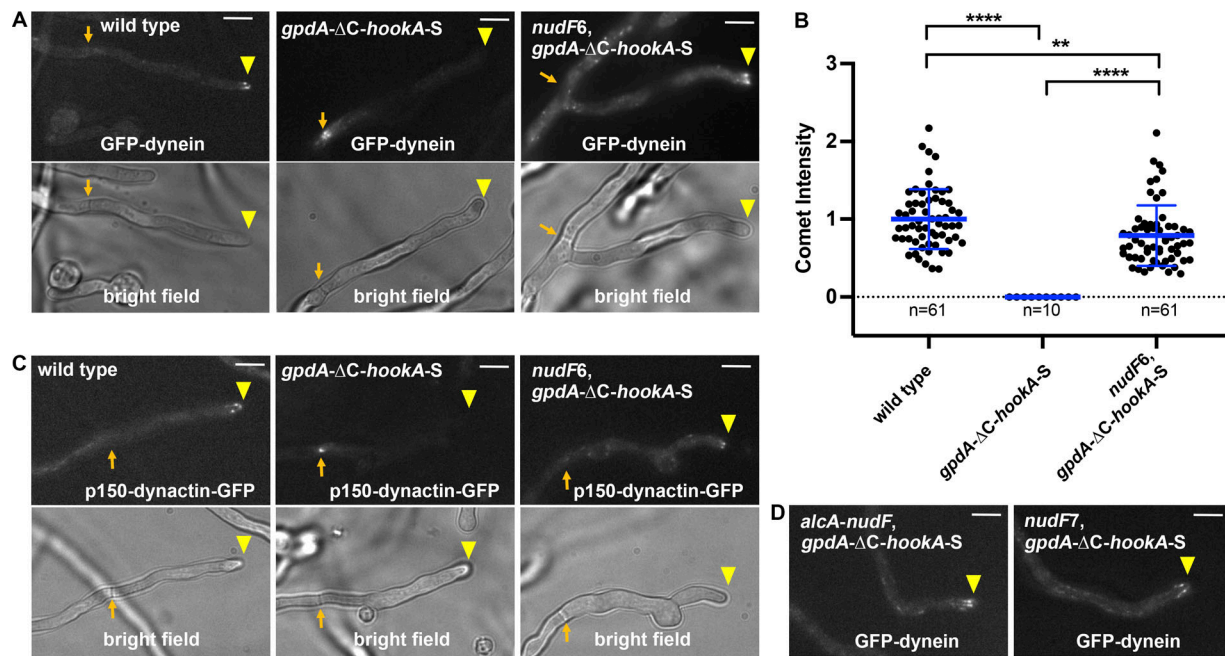
we were only able to detect dynein signals at the mitotic spindle poles during anaphase (Li et al., 2005b). To determine if dynein or dynactin is at the interphase SPBs in ΔC-HookA–overexpressed cells, we used the NLS-DsRed fusion that labels nuclei during interphase (Shen and Osmani, 2013). We found clear SPB-like signals of dynein and dynactin on interphase nuclei in some ΔC-HookA–overexpressed cells (Figs. 1 G and S2 B), which were never observed in wild-type cells. However, the septal signals of dynein–dynactin in the *gpdA*-ΔC-*hookA*-S cells were brighter and more consistently observed than the SPB signals (Fig. S2 C), and thus, we used the septal signals to indicate MT minus-end accumulation in the rest of the work.

The plus-end to minus-end (MTOC) relocation of dynein–dynactin is fully consistent with cargo-adapter–mediated dynein activation observed in vitro (McKenney et al., 2014; Schlager et al., 2014; Olenick et al., 2016; Schroeder and Vale, 2016; Baumbach et al., 2017; Jha et al., 2017). In the budding yeast, dynein also uses its motor activity to move from the plus end toward the minus end upon overexpression of the coiled-coil domain of the cortical dynein anchor Num1 (Lammers and Markus, 2015). Despite these consistent data, we sought to further confirm that the relocation from the plus end to the minus end needs functional dynein in *A. nidulans*. To do that, we

examined the effect of a previously identified dynein loss-of-function mutation, *nudA*F[208V]. The *nudA*F[208V] mutation in the dynein tail impairs dynein-mediated nuclear distribution and early endosome transport but does not affect dynein–dynactin interaction or dynein–early-endosome interaction (Qiu et al., 2013), consistent with the importance of the tail in dynein motor activity (Ori-McKenney et al., 2010; Rao et al., 2013; Hoang et al., 2017). Upon overexpression of ΔC-HookA, plus-end comets formed by GFP-dynein with the *nudA*F[208V] mutation were still detected (Fig. 1 H), confirming that functional dynein is needed for this relocation.

NudF/LIS1 is required for ΔC-HookA–activated relocation of dynein from the MT plus ends to the minus ends

To examine the role of NudF/LIS1 in ΔC-HookA–mediated dynein activation in vivo, we used the temperature-sensitive *nudF*6 mutant in which the NudF/LIS1 protein is unstable at its restrictive temperature (Xiang et al., 1995a). The *nudF*6 mutation (identified as *nudF*L[304S] in this work) caused a significant defect in ΔC-HookA–activated relocation of dynein and dynactin from the MT plus ends to the septa. Specifically, while the MT plus-end comets formed by dynein or dynactin disappeared and were replaced by the septal accumulation of these proteins in *gpd*

Qiu et al.
LIS1 is required for dynein activation in vivo

Journal of Cell Biology
https://doi.org/10.1083/jcb.201905178

3632

Figure 2.   **NudF/LIS1 is required for the relocation of dynein and dynactin from the MT plus ends to the minus ends upon ΔC-HookA overexpression.**
(A) GFP-dynein in wild type, a *gpdA*-ΔC-*hookA*-S strain, and a *nudF*6, *gpdA*-ΔC-*hookA*-S strain. Note that GFP-dynein accumulates as MT plus-end comets, but not at the septum, in the *nudF*6, *gpdA*-ΔC-*hookA*-S hypha. Bright-field images are shown below to indicate hyphal shape and position of the septum. Hyphal tips are indicated by arrowheads and septa by arrows. **(B)** A quantitative analysis on dynein comet intensity in the *nudF*6, *gpdA*-ΔC-HookA-S strain (*n* = 61) in comparison to those in wild type (*n* = 61) and the *gpdA*-ΔC-HookA-S strain (*n* = 10). The average wild-type value is set as 1. Scatterplots with mean and SD values were generated by Prism 8. ****, P < 0.0001; **, P < 0.01 (Kruskal–Wallis ANOVA test with Dunn's multiple comparisons test, unpaired). **(C)** p150-dynactin-GFP in wild type, a *gpdA*-ΔC-*hookA*-S strain, and a *nudF*6, *gpdA*-ΔC-*hookA*-S strain. Note that GFP-dynactin accumulates as plus-end comets, but not at the septum, in the *nudF*6, *gpdA*-ΔC-*hookA*-S strain. **(D)** GFP-dynein in a *nudF*7, *gpdA*-ΔC-*hookA*-S strain and an *alcA-nudF*, *gpdA*-ΔC-*hookA*-S strain. Note that GFP-dynein plus-end comets are present in these cells. Bars, 5 μm.

A-ΔC-*hookA*-S cells, introducing the *nudF*6 allele into this background caused dynein and dynactin to form plus-end comets instead of the septal accumulation (Fig. 2, A–C). Similar to *nudF*6, another temperature-sensitive mutation, *nudF*7 (Xiang et al., 1995a), and a conditional-null mutation, *alcA-nudF*, which allows NudF/LIS1 expression to be shut off by glucose-mediated repression at the *alcA* promoter (Xiang et al., 1995a), also retained dynein at the MT plus ends upon overexpression of ΔC-HookA (Fig. 2 D). Together, these results indicate that NudF/LIS1 is critically required for ΔC-HookA–mediated dynein activation in *A. nidulans*.

NudF/LIS1 does not accumulate at the MT minus ends upon overexpression of ΔC-HookA

Unlike dynein or dynactin, NudF/LIS1-GFP did not accumulate at septa upon overexpression of ΔC-HookA (Fig. 3 A). Instead, the plus-end comets formed by NudF/LIS1-GFP were still observed upon overexpression of ΔC-HookA. However, the comet intensity was significantly lower than that in wild-type cells, although the NudF/LIS1-GFP protein level was not decreased apparently (Fig. 3, A–C). Thus, ΔC-HookA may drive some NudF/LIS1 proteins to leave the MT plus end with dynein–dynactin, but the association is not maintained. This is consistent with previous studies showing that dynein and dynactin associate with the early endosome undergoing dynein-mediated transport but that LIS1 dissociates from it after the initiation of transport (Lenz et al., 2006; Egan et al., 2012).

Dynein along MTs can be activated by ΔC-HookA to relocate to the minus ends, and NudF/LIS1 is also important for this process

We next sought to address whether dynein can undergo cargo-adapter–mediated activation only at the MT plus ends. In hyphae of *U. maydis*, although many early endosomes start their dynein–dynactin–LIS1–dependent minus-end–directed transport from the MT plus end after being delivered there by kinesin-3 (Lenz et al., 2006), dynein-dependent early endosome transport often initiates in the middle of a MT before the early endosome reaches the plus end (Schuster et al., 2011). In fungi and higher eukaryotic cells, including neurons, plus-end–directed kinesins are required for the accumulation of dynein at the MT plus ends (Zhang et al., 2003; Carvalho et al., 2004; Lenz et al., 2006; Arimoto et al., 2011; Roberts et al., 2014; Twelvetrees et al., 2016). In the Δ*kinA* (Kinesin-1) mutant of *A. nidulans* (Requena et al., 2001), dynein fails to arrive at the MT plus ends but locates along MTs (Zhang et al., 2003, 2010; Egan et al., 2012). We found that GFP-dynein in cells with the Δ*kinA* and *gpdA*-ΔC-*hookA*-S alleles accumulated at septa (Fig. 4 A), suggesting that dynein along MTs can be activated before arriving at the plus ends as long as cargo adapters are available globally. However, adding the *nudF*6 mutation to the genetic background with the Δ*kinA* and *gpdA*-ΔC-*hookA*-S alleles caused the septal accumulation of dynein to be significantly decreased and dynein along MTs to be more obvious (Fig. 4, A and B).
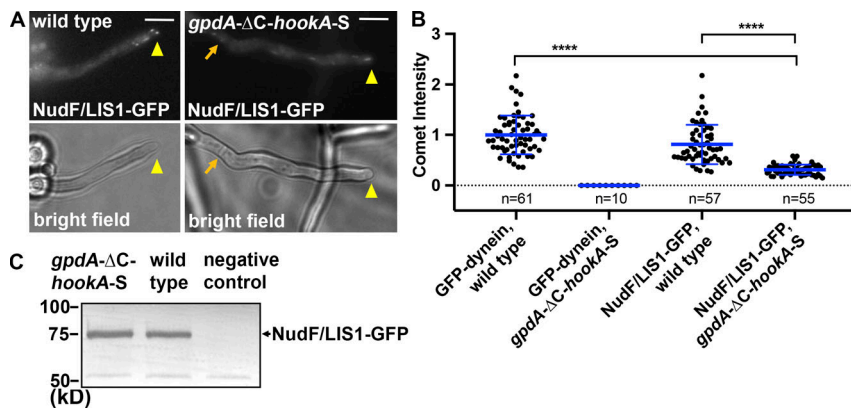
Figure 3. **NudF/LIS1 proteins do not relocate to MT minus ends upon overexpression of ΔC-HookA.** **(A)** NudF/LIS1-GFP signals accumulate as plus-end comets, but not at the septum, in a *gpdA-ΔC-hookA*-S strain. Hyphal tips are indicated by arrowheads and septa by arrows. Bars, 5 µm. **(B)** A quantitative analysis of the NudF/LIS1-GFP comet intensity in wild-type (*n* = 57) and *gpdA-ΔC-hookA*-S (*n* = 55) strains. Two sets of GFP-dynein data (used in Fig. 2 B) were shown for comparison, but only the wild type (*n* = 61) was included in the statistical analysis. The average wild-type value for GFP-dynein is set as 1. Scatterplots with mean and SD values were generated by Prism 8. ****, P < 0.0001 (Kruskal-Wallis ANOVA test with Dunn's multiple comparisons test, unpaired). **(C)** A Western blot showing that the protein level of NudF/LIS1-GFP (arrow) is not changed apparently upon ΔC-HookA overexpression in the *gpdA-ΔC-hookA*-S strain. A strain without the NudF/LIS1-GFP fusion is used as a negative control for the anti-GFP antibody. Note that a nonspecific band slightly above the 50-kD marker helps to show equal loading in the three lanes.

Thus, NudF/LIS1 is important for cargo-adapter–mediated dynein activation even when dynein is not at the MT plus ends. This is consistent with the finding that neuronal LIS1 is important for transport initiation not only in the distal axon containing dynamic MT plus ends but also in the midaxon with much more stable MTs (Moughamian et al., 2013).

The dynein–dynactin–ΔC-HookA complex is still formed without NudF/LIS1

We next used a biochemical pull-down assay to determine if the defect in dynein activation in cells lacking NudF/LIS1 is caused by a defect in the formation of the dynein–dynactin–ΔC-HookA complex. For this assay, we combined the ΔC-HookA-GFP fusion
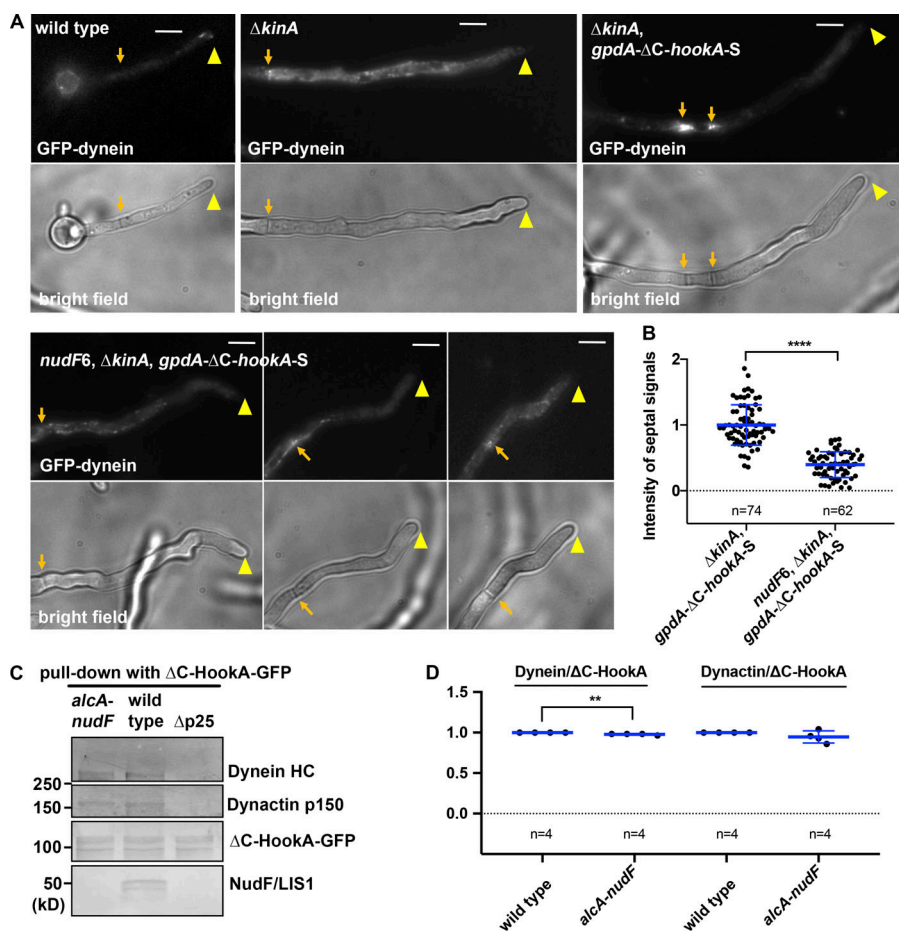
Figure 4. **Dynein along MTs in the ΔkinA mutant relocates to the minus ends upon ΔC-HookA overexpression, and NudF/LIS1 plays an important role in this process. (A)** Images of GFP-dynein in wild type, a *ΔkinA* strain, a *ΔkinA, gpdA-ΔC-hookA*-S strain, and a *nudF*6, *ΔkinA, gpdA-ΔC-hookA*-S strain. Hyphal tips are indicated by arrowheads and septa by brown arrows. Bars, 5 µm. **(B)** A quantitative analysis of septal GFP-dynein signal intensity in *ΔkinA, gpdA-ΔC-hookA*-S (*n* = 74) and *nudF*6, *ΔkinA, gpdA-ΔC-hookA*-S (*n* = 62) strains. The average value for the *ΔkinA, gpdA-ΔC-hookA*-S strain is set as 1. Scatterplots with mean and SD values were generated by Prism 8. ****, P < 0.0001 (Student's *t* test, two-tailed, unpaired). **(C)** Western blots showing that dynein HC and dynactin p150 are pulled down with ΔC-HookA-GFP in wild type and the *alcA-nudF* mutant in which the expression of NudF/LIS1 is shut off. The Δp25 mutant was used as a negative control. **(D)** A quantitative analysis on the ratio of pulled-down dynein HC to ΔC-HookA-GFP (dynein/ΔC-HookA) and that of pulled-down dynactin p150 to ΔC-HookA-GFP (dynactin/ΔC-HookA). The values were generated from western analyses of four independent pull-down experiments (*n* = 4 for all). The wild-type values are set as 1. Scatterplots with mean and SD values were generated by Prism 8. **, P < 0.01 (Student's *t* test, two tailed, unpaired).

Qiu et al.
LIS1 is required for dynein activation in vivo

Journal of Cell Biology
3634
https://doi.org/10.1083/jcb.201905178

under the control of the endogenous *hookA* promoter (Zhang et al., 2014) with the *alcA-nudF* mutant in which NudF/LIS1 expression is shut off by glucose-mediated repression at the *alcA* promoter (Xiang et al., 1995a). The Δp25 mutant was used as a negative control, because p25 of dynactin is important for the formation of the dynein–dynactin–ΔC-HookA complex (Zhang et al., 2014; Qiu et al., 2018). In the *alcA-nudF* mutant, where NudF/LIS1 is undetectable, both dynactin and dynein were still pulled down with ΔC-HookA-GFP, and only a very mild reduction in the ratio of pulled-down dynein to ΔC-HookA compared with that of the wild type was detected (Fig. 4, C and D). Thus, the role of NudF/LIS1 in dynein activation cannot be simply explained by its involvement in the formation of the dynein-dynactin-cargo adapter complex in vivo, suggesting that NudF/LIS1 must be critical for another step of dynein activation.

The phi-opening mutations allow the requirement of NudF/LIS1 to be bypassed to a significant extent

A key step of dynein activation is the switch of dynein from the autoinhibited phi–dynein conformation (Torisawa et al., 2014; Zhang et al., 2017a) to an open conformation that can undergo further activation by dynactin and cargo adapter in vitro to become a processive motor (Zhang et al., 2017a). Formation of phi–dynein depends on interactions between the two dynein HCs, including the ionic interactions between the linker domain and AAA4, and mutating two linker residues opens up phi-dynein (Zhang et al., 2017a). In mammalian cells, dynein with these phi-opening mutations is enriched at centrosomes/spindle poles together with dynactin (Zhang et al., 2017a). To investigate the relationship between phi-dynein and LIS1 function, we constructed an *A. nidulans* strain containing the two analogous phi-opening mutations *nudA*[R1602E, K1645E] (Fig. 5 A). In addition, we also obtained the *nudA*[R1602E] mutant containing only one of the two phi-opening mutations due to a homologous recombination between the two sites. In either case, the wild-type *nudA* allele is replaced by the mutant allele (confirmed by sequencing of the genomic DNA). The *nudA*[R1602E, K1645E] mutant showed a partial defect in nuclear distribution (Fig. S3, A and B), and it formed a colony smaller than wild type, especially at a higher temperature, such as 37°C or 42°C, but the colony phenotype of the *nudA*[R1602E] mutant was not as obvious (Figs. 5 B and S3 C). We also found that combining *gpd*A-ΔC-*hookA*-S with *nudA*[R1602E, K1645E] made the colony almost inviable (Fig. S3 D).

The *nudA*[R1602E, K1645E] mutant exhibited a striking accumulation of GFP-dynein at septa together with mCherry-RabA–labeled early endosomes (Figs. 5 C and S4 A). Interestingly, GFP-dynein with the *nudA*[R1602E] single mutation also accumulated at septa together with early endosomes (Fig. 5 C), suggesting that this mutation must have opened the phi–dynein at least partially.

As the full-length HookA is associated with early endosome, it is most likely that HookA and dynactin activate the open dynein, a notion consistent with the in vitro result that open dynein by itself is not able to walk along the MT processively without dynactin and cargo adapter (Zhang et al., 2017a). By using the Δ*hookA* mutant, we showed that the open dynein is able to localize to the MT plus end. Specifically, we introduced the Δ*hookA* allele into the strain containing *nudA*[R1602E, K1645E] and found bright plus-end

dynein comets in this strain (Fig. S4 B). It is also interesting to note that loss of *hookA* did not fully eliminate the septal dynein accumulation, although it abolished the dynein–early endosome colocalization (Fig. S4 B), consistent with the previously observed movement of early-endosome–free dynein (Schuster et al., 2011). It needs to be addressed in the future whether these septal dynein molecules have been activated by other dynein cargoes whose transport is Hook independent and mediated by adapters waiting to be identified (Peñalva et al., 2017).
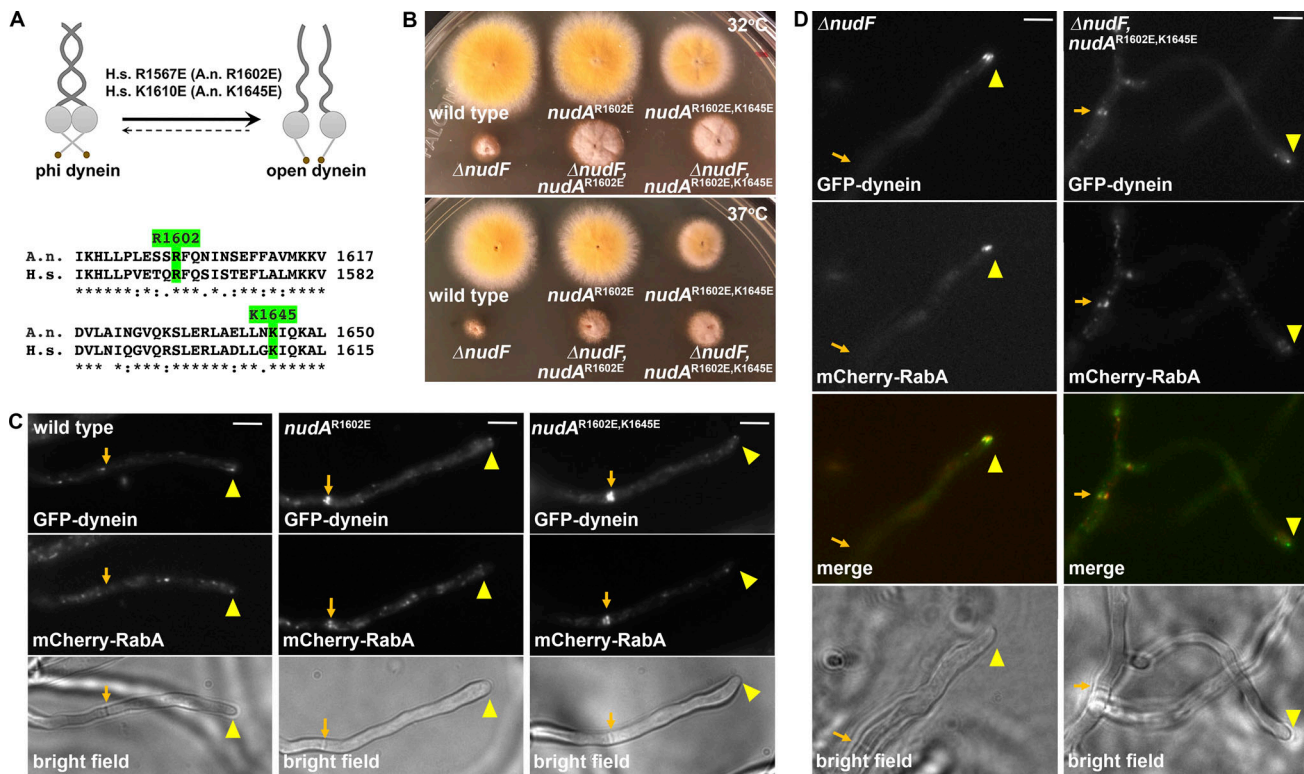
To determine if the phi-opening mutations can bypass NudF/LIS1 function in vivo, we introduced these mutations into the Δ*nudF* (*nudF*-deletion) mutant background. Amazingly, both the *nudA*[R1602E] and *nudA*[R1602E, K1645E] mutations enhanced growth of the Δ*nudF* mutant colony (Fig. 5 B). Moreover, the *nudA*[R1602E, K1645E] mutations allowed dynein and early endosomes to be seen at septa of the Δ*nudF* mutant (Fig. 5 D). Thus, artificially opening phi–dynein allows the requirement of NudF/LIS1 to be partially bypassed. We then performed a more detailed imaging analysis using the temperature-sensitive *nudF*6 mutant containing either *nudA*[R1602E] or *nudA*[R1602E, K1645E] (note that the *nudF*6 mutant is much healthier than Δ*nudF* at a lower temperature, allowing us to obtain enough spores for quantitative imaging). In the *nudF*6 mutant grown at its restrictive temperature, GFP-dynein with *nudA*[R1602E] mainly formed plus-end comets, but GFP-dynein with *nudA*[R1602E, K1645E] accumulated at septa together with early endosomes, even though plus-end comets did not completely disappear (Fig. 6, A–C). This result suggests that the *nudA*[R1602E] single mutation must have only opened phi–dynein partially and is not able to compensate for the loss of NudF/LIS1 as effectively as the *nudA*[R1602E, K1645E] allele.

It was found previously that phi opening enhances the formation of the mammalian dynein–dynactin–cargo-adapter complex in vitro (Zhang et al., 2017a). To determine if this happens in *A. nidulans*, we performed a biochemical pull-down assay using strains carrying GFP-dynein with the phi-opening mutations and the ΔC-HookA-S fusion expressed under the control of the endogenous *hookA* promoter. Interestingly, both *nudA*[R1602E] and *nudA*[R1602E, K1645E] caused an increase in the amount of ΔC-HookA pulled down with GFP-dynein, although the increase caused by *nudA*[R1602E] is slightly less significant than that caused by *nudA*[R1602E, K1645E] (Fig. 6, D and E). In addition, *nudA*[R1602E, K1645E] caused a mild increase in the amount of dynactin pulled down with GFP-dynein, but no significant change in the amount of NudF/LIS1 pulled down was detected (Fig. 6, D and E).

Importantly, upon overexpression of ΔC-HookA, GFP-dynein with *nudA*[R1602] accumulated at septa in the *nudF*6 background, which is in sharp contrast to the plus-end accumulation of wild-type dynein in the same genetic background (Fig. 7, A and B). This result suggests that the cargo adapter works synergistically with the partial phi-opening mutation to overcome the inhibition in dynein activation caused by loss of NudF/LIS1.

NudE is required for dynein activation and its loss is partially compensated by the phi-opening mutations

Previous studies have suggested a role of NudE in enhancing LIS1 function by recruiting LIS1 to dynein (Efimov, 2003; Shu

Qiu et al.
LIS1 is required for dynein activation in vivo

Journal of Cell Biology   3635
https://doi.org/10.1083/jcb.201905178

Figure 5. Phi opening allows NudF/LIS1 function to be partially bypassed. (A) A cartoon showing the phi-opening mutations (Zhang et al., 2017a) and a sequence alignment of corresponding dynein HC regions from human (H.s.) and *A. nidulans* (A.n.). **(B)** Colony phenotypes of phi-opening mutants and suppression of the Δ*nudF* growth defect by the phi-opening mutations at 32°C and 37°C. **(C)** GFP-dynein with *nudA*R1602E or *nudA*R1602E, K1645E accumulates at septa with early endosomes (mCherry-RabA), while GFP-dynein in the wild-type *nudA* background forms MT plus-end comets. Hyphal tips are indicated by arrowheads and septa by arrows. **(D)** Images of GFP-dynein and mCherry-RabA in Δ*nudF* and Δ*nudF*, *nudA*R1602E, K1645E strains. Note that GFP-dynein with *nudA*R1602E, K1645E is able to accumulate at septa with mCherry-RabA in the absence of NudF/LIS1. Bars, 5 μm.

et al., 2004; Li et al., 2005a; McKenney et al., 2010; Zyłkiewicz et al., 2011; Wang et al., 2013). However, NudE was also thought to relieve the inhibition of LIS1 on dynein motility (Yamada et al., 2008). More interestingly, NudE and the p150 subunit of dynactin both bind to the N-terminus of dynein intermediate chain and may compete for the binding site (Karki and Holzbaur, 1995; Vaughan and Vallee, 1995; King et al., 2003; McKenney et al., 2011; Wang et al., 2013; Jie et al., 2017). The role of NudE in cargo-adapter–mediated dynein activation has never been addressed in vivo or in vitro. To address this, we first introduced GFP-dynein and the *gpdA*-ΔC-*hookA*-S allele into the Δ*nudE* background. We found that although overexpression of ΔC-HookA drives dynein relocation from the MT plus ends to the minus ends, this does not happen in the Δ*nudE* mutant (Fig. 8 A). Thus, just like NudF/LIS1, NudE is also required for cargo-adapter–mediated dynein activation.

Furthermore, we found that the phi-opening mutations of dynein allow the function of NudE to be bypassed to a significant extent. In the Δ*nudE* mutant, dynein accumulates at the MT plus end as shown previously (Efimov, 2003), and mCherry-RabA–labeled early endosomes accumulate abnormally at the hyphal tip (Fig. 8 B), as similarly observed upon loss of NudF/LIS1 (Lenz et al., 2006; Zhang et al., 2010; Egan et al., 2012). Importantly, the presence of the phi-opening mutations caused a significant (although not complete) relocation of dynein and

early endosome to the septa in the Δ*nudE* mutant (Fig. 8 B and Fig. S5, A–C). The result that the *nudA*R1602E single mutation allowed a significant septal accumulation of dynein in the Δ*nudE* mutant (Figs. 8 B and S5 C), but not in the *nudF*6 mutant (Fig. 6, A and C), is consistent with the notion that the function of NudF/LIS1 is only partially lost upon loss of NudE in fungi (Efimov and Morris, 2000; Li et al., 2005a; Efimov et al., 2006).

Discussion

In this study, we developed a robust in vivo assay for cargo-adapter–mediated dynein activation, which allowed us to dissect the function and mechanism of the dynein regulator NudF/LIS1 (called LIS1 hereafter). We found that both LIS1 and its binding protein, NudE, are critical for cargo-adapter–mediated dynein activation in vivo. Remarkably, the requirement for LIS1 or NudE in vivo is bypassed to a significant extent if the auto-inhibited phi–dynein is opened up artificially. Our results provide the in vivo evidence to suggest that LIS1–NudE may promote the opening of phi–dynein, a key step of dynein activation.

LIS1 is required for cytoplasmic dynein function in many different cell types (Kardon and Vale, 2009; Vallee et al., 2012; Olenick and Holzbaur, 2019). Possibly, it also regulates dynein inside cilia/flagella, where dynactin is absent, since LIS1 is
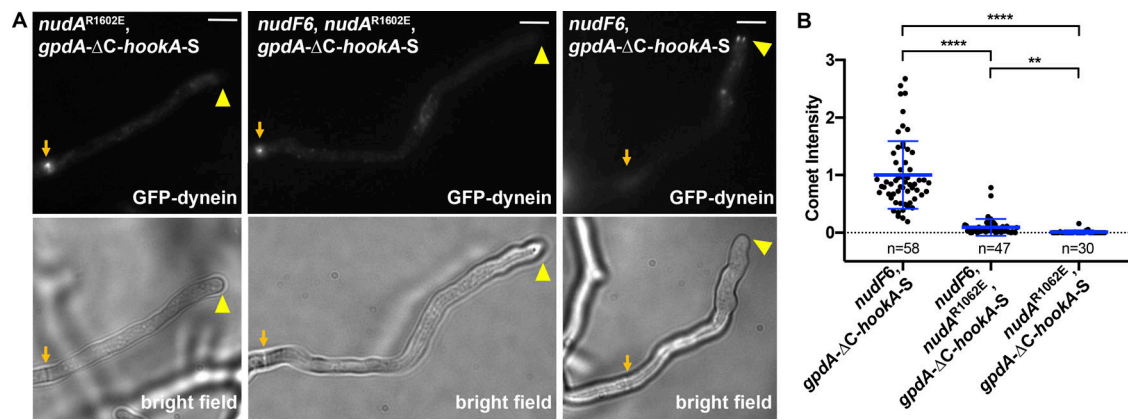
Qiu et al.
LIS1 is required for dynein activation in vivo

Journal of Cell Biology 3636
https://doi.org/10.1083/jcb.201905178
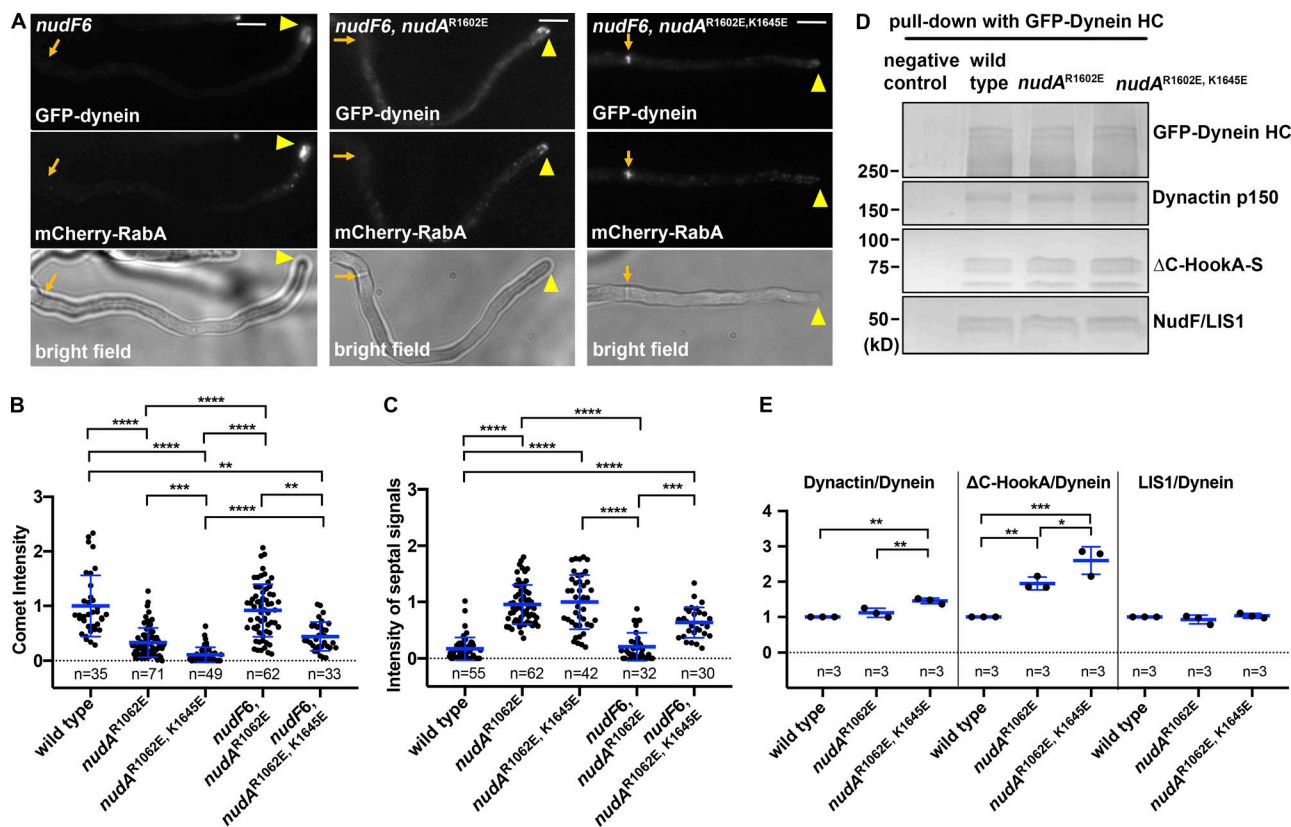
Figure 6. **Phi opening partially compensates for NudF/LIS1 deficiency and mildly enhances the formation of the dynein–dynein–ΔC-HookA complex.** **(A)** Images of GFP-dynein and mCherry-RabA in a *nudF*6 strain, a *nudF*6, *nudA*[R1602E] strain, and a *nudF*6, *nudA*[R1602E, K1645E] strain. Hyphal tips are indicated by arrowheads and septa by arrows. Note that GFP-dynein with *nudA*[R1602E, K1645E] accumulates at a septum with early endosomes (mCherry-RabA) in the *nudF*6 mutant. **(B)** A quantitative analysis on GFP-dynein comet intensity in wild-type ($n = 35$), *nudA*[R1602E] ($n = 71$), *nudA*[R1602E, K1645E] ($n = 49$), *nudF*6, *nudA*[R1602E] ($n = 62$), and *nudF*6, *nudA*[R1602E, K1645E] ($n = 33$) strains. The average value for wild type is set as 1. **(C)** A quantitative analysis on septal dynein intensity in wild-type ($n = 55$), *nudA*[R1602E] ($n = 62$), *nudA*[R1602E, K1645E] ($n = 42$), *nudF*6, *nudA*[R1602E] ($n = 32$), and *nudF*6, *nudA*[R1602E, K1645E] ($n = 30$) strains. The average value for the *nudA*[R1602E, K1645E] strain is set as 1. For both B and C, scatterplots with mean and SD values were generated by Prism 8. ****, $P < 0.0001$; ***, $P < 0.001$; **, $P < 0.01$ (Kruskal–Wallis ANOVA test with Dunn's multiple comparisons test, unpaired). **(D)** Western blots showing the effects of the *nudA*[R1602E] and *nudA*[R1602E, K1645E] mutations on dynein–dynein–ΔC-HookA complex formation. A ΔC-*hookA*-S strain without GFP-dynein was used as a negative control. **(E)** A quantitative analysis on the ratios of pulled-down dynactin p150, ΔC-HookA-S, and NudF/LIS1 to GFP-dynein HC, indicated as Dynactin/Dynein, ΔC-HookA/Dynein, and LIS1/Dynein, respectively. The values were generated from western analyses of three independent pull-down experiments ($n = 3$ for all). The wild-type values are set as 1. Scatterplots with mean and SD values were generated by Prism 8. ***, $P < 0.001$; **, $P < 0.01$; *, $P < 0.05$ (one-way ANOVA, unpaired).

associated with outer-arm dynein required for flagellar beating, and the intraflagella transport dynein-2 is regulated by a phi-like autoinhibited state (Pedersen et al., 2007; Rompolas et al., 2012; Toropova et al., 2017; Roberts, 2018). Our results on the positive role of LIS1 in dynein activation are consistent with the results that LIS1 enhances the speed and/or frequency of dynein motility to varying extents in different in vitro motility assays in the presence of dynactin and the N-terminal portion of the cargo adapter BicD2 (Baumbach et al., 2017; Gutierrez et al., 2017; Jha et al., 2017). Nevertheless, the results from *A. nidulans* are more striking. While the dynein–dynactin–cargo-adapter complex moves robustly toward the MT minus end in the absence of LIS1 in vitro (McKenney et al., 2014; Schlager et al., 2014), LIS1 is critical for the ΔC-HookA–activated dynein relocation in vivo. We postulate that the intracellular environment may require dynein to operate under higher tension and with more complicated regulations. For example, tension applied to the dynein linker domain in vitro alters the regulatory requirement for

dynein motility (Nicholas et al., 2015), as revealed during analyzing the AAA3 domain of dynein (Bhabha et al., 2014; DeWitt et al., 2015; Nicholas et al., 2015).

In *A. nidulans*, dynein carrying the phi-opening mutations dramatically accumulates at septal MTOCs with early endosomes, suggesting that opening the phi–dynein must have allowed dynein to bind more robustly to dynactin and cargo adapter (Fig. 6, D and E; Zhang et al., 2017a) and/or switch to the active conformation more effectively after cargo binding. Interestingly, only the two mutations that open phi–dynein more completely can partially bypass the requirement of LIS1 function to allow dynein to be accumulated at the septa. However, the single *nudA*[R1602E] mutation, which presumably opens phi–dynein incompletely, also allows the requirement of LIS1 for dynein activation to be partially bypassed when ΔC-HookA is overexpressed. Thus, binding of cargo adapter can further promote the open state of dynein to compensate for LIS1 loss. This is consistent with the model that dynactin and cargo adapter

Qiu et al.
LIS1 is required for dynein activation in vivo

Journal of Cell Biology
https://doi.org/10.1083/jcb.201905178

3637

Figure 7. The *nudA*^R1602E mutation causes GFP-dynein to accumulate at the septa in *gpdA-ΔC-hookA*-S cells regardless of NudF/LIS1 function. **(A)** GFP-dynein with the *nudA*^R1602E mutation accumulates at the septa in *gpdA-ΔC-hookA*-S cells with or without the *nudF6* mutation. Hyphal tips are indicated by arrowheads and septa by arrows. **(B)** A quantitative analysis on dynein comet intensity in *nudF6, gpdA-ΔC-hookA*-S (n = 58), *nudF6, nudA*^R1602E, *gpdA-ΔC-hookA*-S (n = 47), and *nudA*^R1602E, *gpdA-ΔC-hookA*-S (n = 30) strains. The average value for the *nudF6, gpdA-ΔC-hookA*-S strain is set as 1. Scatterplots with mean and SD values were generated by Prism 8. ****, P < 0.0001; **, P < 0.01 (Kruskal-Wallis ANOVA test with Dunn's multiple comparisons test, unpaired).

further switch dynein to the active state, thereby preventing the equilibrium from being shifted toward the phi state (Zhang et al., 2017a). Without dynactin and cargo adapter, LIS1 may still promote the open state, but dynein would not be fully functional to move along MTs (Zhang et al., 2017a). Both phi opening and LIS1 promote the dynein–dynactin–cargo-adapter complex formation in vitro (Baumbach et al., 2017; Zhang et al., 2017a), and LIS1 also enhances the dynein–dynactin interaction in *Drosophila melanogaster* and *Xenopus laevis* egg extracts (Dix et al., 2013; Wang et al., 2013). However, this role of LIS1 is not obvious in *A. nidulans* in the presence of the cytosolic ΔC-HookA expressed under the control of *hookA*'s endogenous promoter (Fig. 4, C and D). It is possible that the concentrations of ΔC-HookA, the dynein complex, and the dynactin complex in *A. nidulans* are high enough to allow the formation of the dynein–dynactin–ΔC-HookA complex without LIS1. Together, our results suggest that promoting the switch from the auto-inhibited phi–dynein to open dynein rather than enhancing the dynein–dynactin–cargo-adapter complex formation per se is one key function of LIS1 in *A. nidulans* (Fig. 9).

Recently, LIS1's role in promoting the switch from phi–dynein to open dynein has also been supported by results from in vitro and yeast genetic studies, and structural studies further suggest that the binding of LIS1 to the dynein motor domain at AAA3/AAA4 and/or stalk stabilizes the open dynein (Huang et al., 2012; Toropova et al., 2014; DeSantis et al., 2017; Zhang et al., 2017a; Elshenawy et al., 2019 *Preprint*; Olenick and Holzbaur, 2019; Htet et al., 2019 *Preprint*; Marzo et al., 2019 *Preprint*). This function of LIS1 would in turn facilitate the cargo-adapter–dynactin–mediated switch of dynein to a fully functional state with the two dynein HCs being in a parallel configuration (Zhang et al., 2017a). Interestingly, the LIS1-binding protein NudE is also required for dynein activation in vivo, and the requirement of NudE is also bypassed to a significant extent by the phi-opening mutations. This is consistent with the notion that NudE enhances LIS1 function. NudE binds to the dynein intermediate chain in the dynein tail, a site also

required for dynactin binding (McKenney et al., 2011; Wang et al., 2013; Jie et al., 2017). As the two dynein tails are held together at several positions in the phi–dynein conformation (Fig. 9; Zhang et al., 2017a), it cannot be excluded that NudE may participate in phi opening from the tail side to promote LIS1 function. However, because overexpression of LIS1 totally compensates for the loss of NudE (Efimov, 2003), we favor the possibility that NudE is not directly involved in phi opening but simply helps bring LIS1 close to its site of action.

Since the two phi-opening mutations allow LIS1 function to be bypassed to a significant extent, but not completely, we would not rule out the possibility that LIS1 has additional roles in dynein regulation besides shifting phi–dynein toward an open conformation. This is agreeable with recent data from other laboratories, which are consistent with LIS1's role in promoting the open conformation of dynein but show that the function of LIS1 is not fully mimicked by the phi-opening mutations (Elshenawy et al., 2019 *Preprint*; Htet et al., 2019 *Preprint*; Marzo et al., 2019 *Preprint*). We should also point out that constitutively opening up phi–dynein as achieved by the phi-opening mutations has a clear negative effect inside cells, as it causes mitotic defects in mammalian cells (Zhang et al., 2017a) and a defect in nuclear distribution in *A. nidulans* (Fig. S3, A and B). Thus, phi opening must be regulated for normal dynein function in vivo, and identification of the regulatory factors will be an important task in the future.

One important issue is the spatial regulation of dynein activation mediated by dynactin, cargo adapter, and LIS1 in cells. In fungal hyphae, dynein and dynactin accumulate at the MT plus end before interacting with cargo adapters, and the plus-end accumulation of LIS1 should facilitate dynein activation at the plus end. However, although the MT plus end has been considered as a cargo-loading site in various cell types (Vaughan et al., 2002; Lenz et al., 2006; Lomakin et al., 2009; Moughamian et al., 2013), dynein molecules along a MT may also be involved in cargo-adapter–mediated dynein activation that needs dynactin and LIS1 (Schuster et al., 2011; Moughamian et al., 2013).
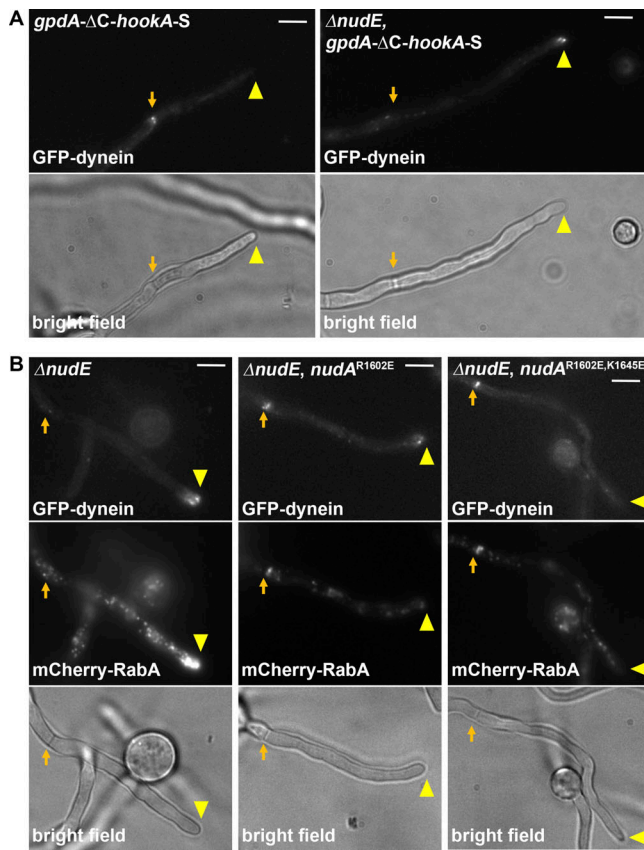
Figure 8. **NudE is required for dynein activation, and phi opening allows the function of NudE to be partially bypassed. (A)** GFP-dynein in *gpdA-ΔC-hookA*-S and *ΔnudE, gpdA-ΔC-hookA*-S strains. Note that GFP-dynein accumulates as MT plus-end comets near the hyphal tip (yellow arrowheads), but not at the septum (arrows), in the *ΔnudE, gpdA-ΔC-hookA*-S strain. **(B)** GFP-dynein and mCherry-RabA in a *ΔnudE* strain, a *ΔnudE, nudA*R1602E strain, and a *ΔnudE, nudA*R1602E, K1645E strain. Note that GFP-dynein with *nudA*R1602E or *nudA*R1602E, K1645E accumulates at the septum with early endosomes (mCherry-RabA) in the absence of NudE. Bars, 5 μm.

Figure 9. A model of LIS1 function in cargo-adapter-mediated dynein activation. Based on our result that the dynein–dynactin–ΔC-HookA complex is still formed without LIS1, we propose that between the fully closed (phi) and open states of dynein, there is an intermediate state in which the dynein tails are partially separated to allow the interactions with dynactin and cargo adapters. However, this complex is not functional in vivo without LIS1. Based on our result that the phi-opening mutations mimic LIS1 function to a significant extent, we propose that LIS1 shifts the equilibria toward the open state and then the fully functional state where the two HCs within the dimer are parallel to each other (Zhang et al., 2017a). This functional state may have a relatively weak affinity for LIS1 to allow its dissociation from the complex at some point during the minus-end–directed movement.

In this study, we show that the LIS1-involved dynein activation may also occur before dynein and dynactin are transported to the MT plus end by kinesin-1 when cytosolic cargo adapters are globally available (Fig. 4, A and B). In this scenario, some dynein or dynein-dynactin complexes may be bound to LIS1 before reaching the plus end. The interaction between LIS1 and dynein appears quite dynamic. LIS1 could fall off the motile dynein–dynactin–cargo-adapter complex as suggested by previous studies (Lenz et al., 2006; Egan et al., 2012; Jha et al., 2017) and recent data (Fig. 3, A-C; Elshenawy et al., 2019 *Preprint*; Htet et al., 2019 *Preprint*), although a more stable association with the motile complex has also been observed (Baumbach et al., 2017; Gutierrez et al., 2017). What regulates LIS1's interaction with dynein during its movement needs to be further addressed.

During this work, we found an intriguing phenomenon that the septal MTOCs in *A. nidulans* are more consistently occupied with activated dynein than the SPBs. A previous study has suggested that the SPB-generated MTs in *A. nidulans* are tyrosinated and unstable during mitosis whereas the detyrosinated MTs are stable and possibly generated from the septal
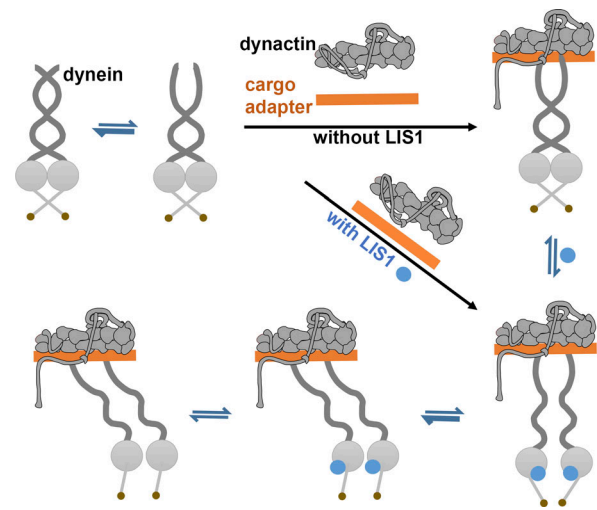
MTOCs (Zekert and Fischer, 2009). It would be worthwhile to further determine whether MTs from these MTOCs are modified differently, which may potentially affect MT length/stability and/or the interaction with dynein at the minus ends. Indeed, tyrosination/detyrosination affects the interaction of dynein–dynactin or kinesin-3 with MTs, although the mechanisms may not be conserved and the details differ in different organisms (Zekert and Fischer, 2009; Seidel et al., 2013; Steinberg, 2015; McKenney et al., 2016; Nirschl et al., 2016; Tas et al., 2017).

Materials and methods
Strains, media, and live-cell imaging
A. nidulans strains used in this study are listed in Table 1. Genetic crosses were done by standard methods, and progeny with desired genotypes were selected based on colony phenotype, imaging analysis, Western analysis, diagnostic PCR, and/or sequencing of specific regions of the genomic DNA. All images were captured using an Olympus IX73 inverted fluorescence microscope linked to a PCO/Cooke Corporation Sensicam QE cooled charge coupled device camera. A UPlanSApo 100× objective lens (oil) with a 1.40 numerical aperture was used. A filter-wheel system with GFP/mCherry-ET Sputtered series with high transmission (Biovision Technologies) was used. IPLab software was used for image acquisition and analysis. Image labeling was done using Microsoft PowerPoint and/or Adobe Photoshop. Quantitation of signal intensity was done as

Table 1. **A. nidulans strains used in this study**

Strain	Genotype	Source
RQ2	GFP-nudA[HC]; argB2::[argB*-alcAp::mCherry-RabA]; ΔnkuA::argB; pyrG89; pyroA4; yA2	Qiu et al., 2013
RQ54	argB2::[argB*-alcAp::mCherry-RabA]; ΔnkuA::argB; pyrG89; pyroA4; wA2	Qiu et al., 2013
RQ128	ΔC-hookA-S-AfpyrG; argB2::[argB*-alcA(p)::mCherry-RabA]; pyrG89; ΔnkuA::argB pyroA4; wA2	Qiu et al., 2018
RQ137	GFP-nudA[HC]; ΔC-hookA-S-AfpyrG; argB2::[argB*-alcA(p)::mCherry-RabA]; possibly pyrG89; possibly ΔnkuA::argB; pabaA1	Qiu et al., 2018
JZ569	ΔC-hookA-GFP-AfpyrG; argB2::[argB*-alcA(p)::mCherry-RabA]; ΔnkuA::argB; pyrG89; pyroA4; wA2	Zhang et al., 2014
XY13	p150-GFP-AfpyrG; ΔnkuA::argB; pyrG89; pyroA4	Yao et al., 2012
JZ383	ΔnudF-pyr4; GFP-nudA[HC]; argB2::[argB*-alcAp::mCherry-RabA]	This work
JZ641	Δp25-AfpyrG; ΔC-hookA-GFP-AfpyrG; argB2::[argB*-alcAp::mCherry-RabA]; possibly pyrG89; possibly ΔnkuA::argB; wA2	This work
JZ878	alcA(p)::nudF-pyr4, chaA1; ΔC-hookA-GFP-AfpyrG; argB2::[argB*-alcA(p)::mCherry-RabA]; possibly ΔnkuA::argB; pyrG89	This work
RQ165	NudF-GFP-AfpyrG; argB2::[argB*-alcAp::mCherry-RabA]; ΔnkuA::argB; pyrG89; pyroA4; yA2	This work
RQ247	gpdA-ΔC-hookA-S-AfpyrG; argB2::[argB*-alcAp::mCherry-RabA]; ΔnkuA::argB; pantoB100; yA2	This work
RQ231	gpdA-ΔC-hookA-S-AfpyrG; hhoA-GFP-AfriboB; argB2::[argB*-alcAp::mCherry-RabA]; pyrG89; pantoB100; ΔnkuA::argB	This work
RQ232	ΔC-hookA-S-AfpyrG; hhoA-GFP-AfriboB; argB2::[argB*-alcAp::mCherry-RabA]; pyrG89; pantoB100; ΔnkuA::argB	This work
RQ265	p150-GFP-AfpyrG; ΔyA::NLS-DsRed; gpdA-ΔC-hookA-S-AfpyrG; possibly pyrG89; possibly ΔnkuA::argB	This work
RQ270	gpdA-ΔC-hookA-S-AfpyrG; ΔyA::NLS-DsRed	This work
RQ271	ΔC-hookA-S-AfpyrG; ΔyA::NLS-DsRed	This work
RQ274	nudF6; GFP-nudA[HC]; pyrG89; yA2; possibly ΔnkuA::argB	This work
RQ275	nudF6; gpdA-ΔC-hookA-S-AfpyrG; GFP-nudA[HC]; pyrG89; yA2; possibly ΔnkuA::argB	This work
RQ276	gpdA-ΔC-hookA-S-AfpyrG; GFP-nudA[HC]; ΔyA::NLS-DsRed	This work
RQ278	gpdA-ΔC-hookA-S-AfpyrG; p150-GFP-AfpyrG; ΔnkuA::argB; pyrG89	This work
RQ285	GFP-nudA[HC]; ΔkinA::pyr4; gpdA-ΔC-hookA-S-AfpyrG; yA2	This work
RQ286	GFP-nudA[HC]; ΔkinA::pyr4; yA2	This work
RQ287	GFP-nudA[HC]; gpdA-ΔC-hookA-S-AfpyrG; yA2	This work
RQ288	hookA-S-AfpyrG; hhoA-GFP-AfriboB; argB2::[argB*-alcAp::mCherry-RabA]; pyrG89; pantoB100; ΔnkuA::argB	This work
RQ290	GFP-nudA[R1602E]; argB2::[argB*-alcAp::mCherry-RabA]; ΔnkuA::argB; pyroA4; yA2	This work
RQ294	GFP-nudA[R1602E, K1645E]; argB2::[argB*-alcAp::mCherry-RabA]; ΔnkuA::argB; pyroA4; yA2	This work
XX357	hhoA-GFP-AfriboB; argB2::[argB*-alcAp::mCherry-RabA]; pyrG89; pantoB100; ΔnkuA::argB	This work
XX358	ΔyA::NLS-DsRed; pyrG89; pryoA4; possibly ΔnkuA::argB	This work
XX483	p150-GFP-AfpyrG; ΔyA::NLS-DsRed; possibly pyrG89; possibly ΔnkuA::argB	This work
XX491	nudF6; gpdA-ΔC-hookA-S-AfpyrG; p150-GFP-AfpyrG; possibly pyrG89; possibly ΔnkuA::argB	This work
XX509	nudF7; gpdA-ΔC-hookA-S-AfpyrG; GFP-nudA[HC]; pyrG89; yA2; possibly ΔnkuA::argB	This work
XX514	GFP-nudA[HC]; ΔyA::NLS-DsRed; possibly ΔnkuA::argB	This work
XX536	gpdA-ΔC-hookA-S-AfpyrG; ΔyA::NLS-DsRed; pantoB100	This work
XX546	alcAp-nudF-pyr4, gpdA-ΔC-hookA-S-AfpyrG; GFP-nudA[HC]; yA2; possibly pyrG89; possibly ΔnkuA::argB	This work
XX551	clipA-mCherry::AfpyroA; gpdA-ΔC-hookA-S-AfpyrG; GFP-nudA[HC]; possibly pyrG89; possibly ΔnkuA::argB	This work
XX565	GFP-nudA[F208V]; gpdA-ΔC-hookA-S-AfpyrG; argB2::[argB*-alcAp::mCherry-RabA]; pyrG89; possibly wA2; possibly yA2; possibly ΔnkuA::argB	This work
XX566	nudF-GFP-AfpyrG; gpdA-ΔC-hookA-S-AfpyrG; argB2::[argB*-alcAp::mCherry-RabA]; wA2	This work
XX571	ΔnudE::argB; GFP-nudA[HC]; pyrG89; yA2	This work
XX572	ΔnudE::argB; GFP-nudA[HC]; gpdA-ΔC-hookA-S-AfpyrG; pyrG89; possibly ΔnkuA::argB	This work
XX579	nudF6; GFP-nudA[HC]; ΔkinA::pyr4; gpdA-ΔC-hookA-S-AfpyrG; possibly pyrG89; possibly ΔnkuA::argB	This work
XX581	nudF6; GFP-nudA[R1602E]; argB2::[argB*-alcAp::mCherry-RabA]; yA2; possibly ΔnkuA::argB	This work
XX597	nudF6; GFP-nudA[HC]; argB2::[argB*-alcAp::mCherry-RabA]; yA2; possibly ΔnkuA::argB	This work
XX598	nudF6; GFP-nudA[R1602E]; gpdA-ΔC-hookA-S-AfpyrG; possibly pyrG89; possibly ΔnkuA::argB	This work

Qiu et al.
LIS1 is required for dynein activation in vivo

Journal of Cell Biology 3640
https://doi.org/10.1083/jcb.201905178

Table 1. *A. nidulans* strains used in this study (*Continued*)

Strain	Genotype	Source
XX599	GFP-*nudA*[R1602E]; *gpdA-ΔC-hookA-S-AfpyrG*; *possibly pyrG89*; *possibly ΔnkuA::argB*	This work
XX609	*nudF6*, GFP-*nudA*[R1602E, K1645E]; *argB2::[argB*-alcAp::mCherry-RabA]*; *possibly ΔnkuA::argB*; *yA2*	This work
XX614	GFP-*nudA*[R1602E, K1645E]; *ΔhookA-AfpyrG*; *argB2::[argB*-alcAp::mCherry-RabA]*; *possibly ΔnkuA::argB*; *yA2*	This work
XX620	*ΔnudE::argB*; GFP-*nudA*[R1602E, K1645E]; *argB2::[argB*-alcAp::mCherry-RabA]*; *possibly ΔnkuA::argB*; *yA2*	This work
XX623	*ΔnudE::argB*; GFP-*nudA*[R1602E]; *argB2::[argB*-alcAp::mCherry-RabA]*; *possibly ΔnkuA::argB*	This work
XX634	*ΔnudF-pyr4*; GFP-*nudA*[R1602E, K1645E]; *argB2::[argB*-alcAp::mCherry-RabA]*; *possibly ΔnkuA::argB*	This work
XX635	*ΔnudE::argB*; GFP-*nudA*[HC]; *argB2::[argB*-alcAp::mCherry-RabA]*; *yA2*; *possibly ΔnkuA::argB*	This work
XX653	*ΔnudF-pyr4*; GFP-*nudA*[R1602E]; *argB2::[argB*-alcAp::mCherry-RabA]*; *possibly ΔnkuA::argB*	This work
XX655	GFP-*nudA*[R1602E, K1645E]; *ΔC-hookA-S-AfpyrG*; *argB2::[argB*-alcAp::mCherry-RabA]*; *possibly pyrG89*; *possibly ΔnkuA::argB*; *wA2*	This work
XX656	GFP-*nudA*[R1602E]; *ΔC-hookA-S-AfpyrG*; *argB2::[argB*-alcAp::mCherry-RabA]*; *possibly pyrG89*; *possibly ΔnkuA::argB*; *wA2*	This work
XX658	GFP-*nudA*[R1602E, K1645E]; *hhoA-GFP-AfriboB*; *argB2::[argB*-alcAp::mCherry-RabA]*; *ΔnkuA::argB*	This work

described previously (Zhang et al., 2014). Specifically, a region of interest (ROI) was selected and the Max/Min tool of the IPLab program was used to measure the maximal intensity within the ROI. The ROI box was then dragged outside of the cell to take the background value, which was then subtracted from the intensity value. Hyphae were chosen randomly from images acquired under the same experimental conditions. For measuring the signal intensity of a MT plus-end comet formed by GFP-dynein or NudF/LIS1-GFP proteins, only the comet closest to hyphal tip was measured. For measuring GFP-dynein signal intensity at septa, usually only the septum most proximal to the hyphal tip was measured, although sometimes, two septa close to each other in the same hypha were present, in which case both were measured. Images were taken at room temperature immediately after the cells were taken out of the incubators. Cells were cultured overnight in minimal medium with 1% glycerol and supplements at 32°C or 37°C (all experiments using *nudF6* strains and controls were done at 37°C). Note that the *nudF6* mutant is temperature sensitive; it forms a tiny colony lacking asexual spores at a higher temperature (typical of a *nud* mutant), but some spores are produced at its semipermissive temperature of 32°C. Thus, for experiments involving *nudF6*, we harvested spores at 32°C and cultured them at 37°C for imaging analysis. The *nudF6* mutant is much better than *ΔnudF* for imaging analysis, because we can harvest enough spores from the *nudF6* mutant at 32°C, whereas the *ΔnudF* mutant is sick and does not produce spores at any temperature. For a few experiments using strains containing the *alcA-nudF* (conditional null) allele, we harvest spores from the solid minimal medium containing 1% glycerol and cultured them in liquid minimal medium containing 0.1% glucose for imaging analysis. Yeast extract and glucose–rich medium was used for growing cells for protein pull-down experiments.

Constructing the *gpdA-ΔC-hookA-S* strain
For constructing the *gpdA-ΔC-hookA-S* strain, we cotransformed into the *A. nidulans* strain XX357 the fragment containing ΔC-hookA-S-AfpyrG (Zhang et al., 2018) with another fragment containing the ~1.2-kb *gpdA* promoter inserted in between the

N-terminal HookA coding sequence and its upstream sequence. The *gpdA* promoter was inserted in this region using fusion PCR with primers 41U (5′-CATGCTTGCTTCCTCTTGC-3′), HKpr2 (5′-GGATATGTCCAAGTAATCGCTG-3′), gpdAF2 (5′-CAGCGATTACTTGGACATATCCGACTCGAGTACCATTTAATTCTAT-3′), gpdAR2 (5′-ACGGTACGCTCCGACTCCATTGTGATGTCTGCTCAAGC-3′; these four primers were described previously; Zhang et al., 2014), HKN2 (5′-AGTCGGAGCGTACCGT-3′), and HKgR (5′-TCAGCCTCAAGGTTTTGGTTC-3′). Primers 41U and HKgR were also used for PCR to confirm the correct integration of the *gpdA* promoter in the selected transformants, and overexpression of the ΔC-HookA-S protein was confirmed by western analyses (Figs. 1 B and S1 B).

Constructing the *nudA*[R1602E] and the *nudA*[R1602E, K1645E] dynein HC phi-opening mutants
We used fusion PCR to make a DNA fragment of *nudA* containing both the R1602E and the K1645E mutations using the following primers: 1602F (5′-CGAGCGAGTTCCAGAATATCAACTCAGAATTCTTCG-3′), 1602R (5′-AGTTGATATTCTGGAACTCGCTCGATTCCAGGGGAAGAA-3′), 1645F (5′-GCTGCTTAACGAAATCCAGAAAGCTCTCGGTGAATAC-3′), 1645R (5′-GCTTTCTGGATTTCGTTAAGCAGCTCGGCCAG-3′), NudA54 (5′-GTGGATGAACTCATTCCAAGA-3′), and NudA36 (5′-TTGGATCTACCAGCATAGCCA-3′). The fragment was cotransformed with a selective marker *pyrG* fragment into the RQ2 strain containing GFP-dynein HC (NudA) and mCherry-RabA. More than 200 *pyrG*+ transformants were examined under the microscope, and several of them were selected because they exhibited clear septal enrichment of both the GFP and mCherry signals. Our sequencing analysis indicated that several strains contain both mutations (*nudA*[R1602E, K1645E]), but one strain contains only the *nudA*[R1602E] mutation due to homologous recombination between the two sites.

Constructing the *nudF*-GFP strain
The following oligos were used for fusion PCR to create the *gpdA-nudF*-GFP-*AfpyrG* fragment: F5F (5′-ATCAGACTGGACGAAGCC-3′), F5R (5′-CAAATAGAATTAAATGGTACTCGAGTCGGTTGTTTGTGTTCGCAAAT-3′), gpdF (5′-GACTCGAGTACCATT

Qiu et al.
LIS1 is required for dynein activation in vivo

Journal of Cell Biology
https://doi.org/10.1083/jcb.201905178

3641

TAATTCTATTTG-3′), gpdR (5′-TGTGATGTCTGCTCAAGCG-3′), FF (5′-CGCTTGAGCAGACATCACAATGAGCCAAATATTGAC AGCTCC-3′), FR (5′-GCCTGCACCAGCTCCGCTGAACACCCGTAC AGAGTT-3′), GFPF (5′-GGAGCTGGTGCAGGC-3′), GFPR (5′-CTG TCTGAGAGGAGGCACTG-3′), F3F (5′-CAGTGCCTCCTCTCAGAC AGGTCGCGATCTTCATCACAGTT-3′), and F3R (5′-CGACAGAAT GGAACGGGAAA-3′). This fragment was transformed into the RQ54 strain, and progeny with MT plus-end comets formed by NudF/LIS1-GFP were selected. For this study, we only used a transformant (RQ165) containing NudF-GFP, but not the *gpdA*-NudF-GFP fusion protein.

Biochemical pull-down assays and western analysis

The μMACS GFP-tagged protein isolation kit (Miltenyi Biotec) was used to pull down proteins associated with the GFP-tagged protein. This was done as described previously (Zhang et al., 2014). Specifically, ∼0.4 g of hyphal mass was harvested from overnight culture for each sample, and cell extracts were prepared using a lysis buffer containing 50 mM Tris-HCl, pH 8.0, and 10 μg/ml of a protease inhibitor cocktail (Sigma-Aldrich). Cell extracts were centrifuged at 8,000 *g* for 15 min and then 16,000 *g* for 15 min at 4°C, and supernatant was used for the pull-down experiment. To pull down GFP-tagged proteins, 25 μl anti-GFP MicroBeads was added into the cell extracts for each sample and incubated at 4°C for 30–40 min. The MicroBeads/cell extracts mixture was then applied to the μColumn followed by gentle wash with the lysis buffer used above for protein extraction (Miltenyi Biotec). Preheated (95°C) SDS-PAGE sample buffer was used as elution buffer. Western analyses were performed using the alkaline phosphatase system, and blots were developed using AP color development reagents (Bio-Rad). Quantitation of the protein band intensity was done using IPLab software as described previously (Qiu et al., 2013). Specifically, an area containing the whole band was selected as a ROI, and the intensity sum within the ROI was measured. Then, the ROI box was dragged to the equivalent region of the negative control lane or a blank region without any band on the same blot to take the background value, which was then subtracted from the intensity sum. The rabbit polyclonal antibody against GFP (used for Western blots presented in Figs. 3 C, 4 C, and 6 D) was purchased from Takara Bio (catalog number 632592). The rabbit monoclonal antibody against the S-tag (used for Western blots presented in Figs. 1 B, S1 B, and 6 D) was from Cell Signaling Technology (catalog number 12774S). Polyclonal antibodies against dynein HC (Fig. 4 C), dynactin p150 (Figs. 4 C and 6 D), and NudF/LIS1 (Figs. 4 C and 6 D) were generated in previous studies by injecting proteins produced in bacteria into rabbits followed by affinity purification of the antibodies (Xiang et al., 1995a,b; Zhang et al., 2008).

Statistical analysis

All statistical analyses were done using GraphPad Prism 8 for Mac (version 8.0.0, 2018). The D'Agostino and Pearson normality test was performed on all datasets except Western blot datasets with small *n* (*n* = 3 or *n* = 4). For Western blot data quantitation presented in Fig. 4 D and Fig. 6 E, data distribution was assumed to be normal, but this was not formally

tested. A Student's *t* test (unpaired, two tailed) was used to analyze data in Fig. 4 D, and an ordinary one-way ANOVA (unpaired) was used to analyze data in Fig. 6 E. The datasets presented in Fig. 4 B passed the D'Agostino and Pearson normality test (α = 0.05), and thus, they were analyzed using a Student's *t* test (unpaired, two tailed). For all other datasets, nonparametric tests were used without assuming Gaussian distribution. Specifically, the Kruskal–Wallis ANOVA test (unpaired) with Dunn's multiple comparisons test was used for analyzing multiple datasets presented in Fig. 2 B; Fig. 3 B; Fig. 6, B and C; Fig. 7 B; Fig. S1 D; and Fig. S5, B and C. The Mann–Whitney test (unpaired, two tailed) was used to analyze the two datasets presented in Fig. S3 B. Note that adjusted P values were generated from either the ordinary one-way ANOVA test or the Kruskal–Wallis ANOVA test with Dunn's multiple comparisons test. In all figures, **** indicates P < 0.0001, *** indicates P < 0.001, ** indicates P < 0.01, and * indicates P < 0.05. If the P value is >0.05, the difference is considered not significant, which is not indicated in any figure.

Online supplemental material

Fig. S1 shows a western analysis of the HookA-S and ΔC-HookA-S proteins as well as the partial defect in nuclear distribution caused by ΔC-HookA-S overexpression. Fig. S2 shows the movement of GFP-dynein toward a septum and dynactin localization at the SPBs, with the accumulation of dynein being more obvious at septa than at the SPBs upon ΔC-HookA-S overexpression. Fig. S3 shows the nuclear-distribution and colony-growth phenotypes of the phi-opening mutants of dynein. Fig. S4 shows the accumulation of early endosomes at septa, but not on nuclei, in the phi-opening mutant as well as the localization of open dynein in the Δ*hookA* mutant. Fig. S5 shows a quantitative image analysis on the localization of open dynein in the Δ*nudE* mutant. Video 1 shows the movement of GFP-dynein toward a septum upon ΔC-HookA overexpression.

References

Abenza, J.F., A. Pantazopoulou, J.M. Rodríguez, A. Galindo, and M.A. Peñalva. 2009. Long-distance movement of Aspergillus nidulans early endosomes on microtubule tracks. *Traffic.* 10:57–75. https://doi.org/10.1111/j.1600-0854.2008.00848.x

Akhmanova, A., and J.A. Hammer III. 2010. Linking molecular motors to membrane cargo. *Curr. Opin. Cell Biol.* 22:479–487. https://doi.org/10.1016/j.ceb.2010.04.008

Arimoto, M., S.P. Koushika, B.C. Choudhary, C. Li, K. Matsumoto, and N. Hisamoto. 2011. The Caenorhabditis elegans JIP3 protein UNC-16 functions as an adaptor to link kinesin-1 with cytoplasmic dynein. *J. Neurosci.* 31:2216–2224. https://doi.org/10.1523/JNEUROSCI.2653-10.2011

Asai, D.J., and M.P. Koonce. 2001. The dynein heavy chain: structure, mechanics and evolution. *Trends Cell Biol.* 11:196–202. https://doi.org/10.1016/S0962-8924(01)01970-5

Baumann, S., T. Pohlmann, M. Jungbluth, A. Brachmann, and M. Feldbrügge. 2012. Kinesin-3 and dynein mediate microtubule-dependent co-transport of mRNPs and endosomes. *J. Cell Sci.* 125:2740–2752. https://doi.org/10.1242/jcs.101212

Baumbach, J., A. Murthy, M.A. McClintock, C.I. Dix, R. Zalyte, H.T. Hoang, and S.L. Bullock. 2017. Lissencephaly-1 is a context-dependent regulator of the human dynein complex. *eLife.* 6:e21768. https://doi.org/10.7554/eLife.21768

Bertipaglia, C., J.C. Gonçalves, and R.B. Vallee. 2018. Nuclear migration in mammalian brain development. *Semin. Cell Dev. Biol.* 82:57–66. https://doi.org/10.1016/j.semcdb.2017.11.033

Bhabha, G., H.C. Cheng, N. Zhang, A. Moeller, M. Liao, J.A. Speir, Y. Cheng, and R.D. Vale. 2014. Allosteric communication in the dynein motor domain. *Cell.* 159:857–868. https://doi.org/10.1016/j.cell.2014.10.018

Bielska, E., Y. Higuchi, M. Schuster, N. Steinberg, S. Kilaru, N.J. Talbot, and G. Steinberg. 2014a. Long-distance endosome trafficking drives fungal effector production during plant infection. *Nat. Commun.* 5:5097. https://doi.org/10.1038/ncomms6097

Bielska, E., M. Schuster, Y. Roger, A. Berepiki, D.M. Soanes, N.J. Talbot, and G. Steinberg. 2014b. Hook is an adapter that coordinates kinesin-3 and dynein cargo attachment on early endosomes. *J. Cell Biol.* 204:989–1007. https://doi.org/10.1083/jcb.201309022

Callejas-Negrete, O.A., M. Plamann, R. Schnittker, S. Bartnicki-García, R.W. Roberson, G. Pimienta, and R.R. Mouriño-Pérez. 2015. Two microtubule-plus-end binding proteins LIS1-1 and LIS1-2, homologues of human LIS1 in Neurospora crassa. *Fungal Genet. Biol.* 82:213–227. https://doi.org/10.1016/j.fgb.2015.07.009

Carvalho, P., M.L. Gupta Jr., M.A. Hoyt, and D. Pellman. 2004. Cell cycle control of kinesin-mediated transport of Bik1 (CLIP-170) regulates microtubule stability and dynein activation. *Dev. Cell.* 6:815–829. https://doi.org/10.1016/j.devcel.2004.05.001

DeSantis, M.E., M.A. Cianfrocco, Z.M. Htet, P.T. Tran, S.L. Reck-Peterson, and A.E. Leschziner. 2017. Lis1 Has Two Opposing Modes of Regulating Cytoplasmic Dynein. *Cell.* 170:1197–1208.e12. https://doi.org/10.1016/j.cell.2017.08.037

DeWitt, M.A., C.A. Cypranowska, F.B. Cleary, V. Belyy, and A. Yildiz. 2015. The AAA3 domain of cytoplasmic dynein acts as a switch to facilitate microtubule release. *Nat. Struct. Mol. Biol.* 22:73–80. https://doi.org/10.1038/nsmb.2930

Dix, C.I., H.C. Soundararajan, N.S. Dzhindzhev, F. Begum, B. Suter, H. Ohkura, E. Stephens, and S.L. Bullock. 2013. Lissencephaly-1 promotes the recruitment of dynein and dynactin to transported mRNAs. *J. Cell Biol.* 202:479–494. https://doi.org/10.1083/jcb.201211052

Dwivedi, D., P. Chawla, and M. Sharma. 2019. Incorporating Motility in the Motor: Role of the Hook Protein Family in Regulating Dynein Motility. *Biochemistry.* 58:1026–1031. https://doi.org/10.1021/acs.biochem.8b01065

Efimov, V.P. 2003. Roles of NUDE and NUDF proteins of Aspergillus nidulans: insights from intracellular localization and overexpression effects. *Mol. Biol. Cell.* 14:871–888. https://doi.org/10.1091/mbc.e02-06-0359

Efimov, V.P., and N.R. Morris. 2000. The LIS1-related NUDF protein of Aspergillus nidulans interacts with the coiled-coil domain of the NUDE/RO11 protein. *J. Cell Biol.* 150:681–688. https://doi.org/10.1083/jcb.150.3.681

Efimov, V.P., J. Zhang, and X. Xiang. 2006. CLIP-170 homologue and NUDE play overlapping roles in NUDF localization in Aspergillus nidulans. *Mol. Biol. Cell.* 17:2021–2034. https://doi.org/10.1091/mbc.e05-11-1084

Egan, M.J., K. Tan, and S.L. Reck-Peterson. 2012. Lis1 is an initiation factor for dynein-driven organelle transport. *J. Cell Biol.* 197:971–982. https://doi.org/10.1083/jcb.201112101

Egan, M.J., M.A. McClintock, I.H. Hollyer, H.L. Elliott, and S.L. Reck-Peterson. 2015. Cytoplasmic dynein is required for the spatial organization of protein aggregates in filamentous fungi. *Cell Reports.* 11:201–209. https://doi.org/10.1016/j.celrep.2015.03.028

Elshenawy, M.M., E. Kusakci, S. Volz, J. Baumbach, S.L. Bullock, and A. Yildiz. 2019. Lis1 activates dynein motility by pairing it with dynactin. *bioRxiv.* https://doi.org/10.1101/685826 (Preprint posted June 28, 2019)

Eshel, D., L.A. Urrestarazu, S. Vissers, J.C. Jauniaux, J.C. van Vliet-Reedijk, R.J. Planta, and I.R. Gibbons. 1993. Cytoplasmic dynein is required for normal nuclear segregation in yeast. *Proc. Natl. Acad. Sci. USA.* 90:11172–11176. https://doi.org/10.1073/pnas.90.23.11172

Feng, Y., E.C. Olson, P.T. Stukenberg, L.A. Flanagan, M.W. Kirschner, and C.A. Walsh. 2000. LIS1 regulates CNS lamination by interacting with mNudE, a central component of the centrosome. *Neuron.* 28:665–679. https://doi.org/10.1016/S0896-6273(00)00145-8

Fu, M.M., and E.L. Holzbaur. 2014. Integrated regulation of motor-driven organelle transport by scaffolding proteins. *Trends Cell Biol.* 24:564–574. https://doi.org/10.1016/j.tcb.2014.05.002

Geiser, J.R., E.J. Schott, T.J. Kingsbury, N.B. Cole, L.J. Totis, G. Bhattacharyya, L. He, and M.A. Hoyt. 1997. Saccharomyces cerevisiae genes required in the absence of the CIN8-encoded spindle motor act in functionally diverse mitotic pathways. *Mol. Biol. Cell.* 8:1035–1050. https://doi.org/10.1091/mbc.8.6.1035

Grotjahn, D.A., S. Chowdhury, Y. Xu, R.J. McKenney, T.A. Schroer, and G.C. Lander. 2018. Cryo-electron tomography reveals that dynactin recruits a team of dyneins for processive motility. *Nat. Struct. Mol. Biol.* 25:203–207. https://doi.org/10.1038/s41594-018-0027-7

Guimaraes, S.C., M. Schuster, E. Bielska, G. Dagdas, S. Kilaru, B.R. Meadows, M. Schrader, and G. Steinberg. 2015. Peroxisomes, lipid droplets, and endoplasmic reticulum "hitchhike" on motile early endosomes. *J. Cell Biol.* 211:945–954. https://doi.org/10.1083/jcb.201505086

Guo, X., G.G. Farías, R. Mattera, and J.S. Bonifacino. 2016. Rab5 and its effector FHF contribute to neuronal polarity through dynein-dependent retrieval of somatodendritic proteins from the axon. *Proc. Natl. Acad. Sci. USA.* 113:E5318–E5327. https://doi.org/10.1073/pnas.1601844113

Gutierrez, P.A., B.E. Ackermann, M. Vershinin, and R.J. McKenney. 2017. Differential effects of the dynein-regulatory factor Lissencephaly-1 on processive dynein-dynactin motility. *J. Biol. Chem.* 292:12245–12255. https://doi.org/10.1074/jbc.M117.790048

Han, G., B. Liu, J. Zhang, W. Zuo, N.R. Morris, and X. Xiang. 2001. The Aspergillus cytoplasmic dynein heavy chain and NUDF localize to microtubule ends and affect microtubule dynamics. *Curr. Biol.* 11:719–724. https://doi.org/10.1016/S0960-9822(01)00200-7

Higuchi, Y., P. Ashwin, Y. Roger, and G. Steinberg. 2014. Early endosome motility spatially organizes polysome distribution. *J. Cell Biol.* 204:343–357. https://doi.org/10.1083/jcb.201307164

Hoang, H.T., M.A. Schlager, A.P. Carter, and S.L. Bullock. 2017. DYNC1H1 mutations associated with neurological diseases compromise processivity of dynein-dynactin-cargo adaptor complexes. *Proc. Natl. Acad. Sci. USA.* 114:E1597–E1606. https://doi.org/10.1073/pnas.1620141114

Htet, Z.M., J.P. Gillies, R.W. Baker, A.E. Leschziner, M.E. DeSantis, and S.L. Reck-Peterson. 2019. Lis1 promotes the formation of maximally activated cytoplasmic dynein-1 complexes. *bioRxiv.* https://doi.org/10.1101/683052 (Preprint posted June 27, 2019)

Huang, J., A.J. Roberts, A.E. Leschziner, and S.L. Reck-Peterson. 2012. Lis1 acts as a "clutch" between the ATPase and microtubule-binding domains of the dynein motor. *Cell.* 150:975–986. https://doi.org/10.1016/j.cell.2012.07.022

Jaarsma, D., and C.C. Hoogenraad. 2015. Cytoplasmic dynein and its regulatory proteins in Golgi pathology in nervous system disorders. *Front. Neurosci.* 9:397. https://doi.org/10.3389/fnins.2015.00397

Jha, R., J. Roostalu, N.I. Cade, M. Trokter, and T. Surrey. 2017. Combinatorial regulation of the balance between dynein microtubule end accumulation and initiation of directed motility. *EMBO J.* 36:3387–3404. https://doi.org/10.15252/embj.201797077

Jie, J., F. Lohr, and E. Barbar. 2017. Dynein Binding of Competitive Regulators Dynactin and NudE Involves Novel Interplay between Phosphorylation Site and Disordered Spliced Linkers. *Structure.* 25:421–433.

Qiu et al.
LIS1 is required for dynein activation in vivo

Journal of Cell Biology   3643
https://doi.org/10.1083/jcb.201905178

Kardon, J.R., and R.D. Vale. 2009. Regulators of the cytoplasmic dynein motor. *Nat. Rev. Mol. Cell Biol.* 10:854–865. https://doi.org/10.1038/nrm2804

Karki, S., and E.L. Holzbaur. 1995. Affinity chromatography demonstrates a direct binding between cytoplasmic dynein and the dynactin complex. *J. Biol. Chem.* 270:28806–28811. https://doi.org/10.1074/jbc.270.48.28806

King, S.M. 2000. AAA domains and organization of the dynein motor unit. *J. Cell Sci.* 113:2521–2526.

King, S.J., C.L. Brown, K.C. Maier, N.J. Quintyne, and T.A. Schroer. 2003. Analysis of the dynein-dynactin interaction in vitro and in vivo. *Mol. Biol. Cell.* 14:5089–5097. https://doi.org/10.1091/mbc.e03-01-0025

Klinman, E., and E.L. Holzbaur. 2015. Stress-Induced CDK5 Activation Disrupts Axonal Transport via Lis1/Ndel1/Dynein. *Cell Reports.* 12:462–473. https://doi.org/10.1016/j.celrep.2015.06.032

Konzack, S., P.E. Rischitor, C. Enke, and R. Fischer. 2005. The role of the kinesin motor KipA in microtubule organization and polarized growth of Aspergillus nidulans. *Mol. Biol. Cell.* 16:497–506. https://doi.org/10.1091/mbc.e04-02-0083

Kuijpers, M., D. van de Willige, A. Freal, A. Chazeau, M.A. Franker, J. Hofenk, R.J. Rodrigues, L.C. Kapitein, A. Akhmanova, D. Jaarsma, and C.C. Hoogenraad. 2016. Dynein Regulator NDEL1 Controls Polarized Cargo Transport at the Axon Initial Segment. *Neuron.* 89:461–471. https://doi.org/10.1016/j.neuron.2016.01.022

Lam, C., M.A. Vergnolle, L. Thorpe, P.G. Woodman, and V.J. Allan. 2010. Functional interplay between LIS1, NDE1 and NDEL1 in dynein-dependent organelle positioning. *J. Cell Sci.* 123:202–212. https://doi.org/10.1242/jcs.059337

Lammers, L.G., and S.M. Markus. 2015. The dynein cortical anchor Num1 activates dynein motility by relieving Pac1/LIS1-mediated inhibition. *J. Cell Biol.* 211:309–322. https://doi.org/10.1083/jcb.201506119

Lee, W.L., J.R. Oberle, and J.A. Cooper. 2003. The role of the lissencephaly protein Pac1 during nuclear migration in budding yeast. *J. Cell Biol.* 160:355–364. https://doi.org/10.1083/jcb.200209022

Lenz, J.H., I. Schuchardt, A. Straube, and G. Steinberg. 2006. A dynein loading zone for retrograde endosome motility at microtubule plus-ends. *EMBO J.* 25:2275–2286. https://doi.org/10.1038/sj.emboj.7601119

Li, J., W.L. Lee, and J.A. Cooper. 2005a. NudEL targets dynein to microtubule ends through LIS1. *Nat. Cell Biol.* 7:686–690. https://doi.org/10.1038/ncb1273

Li, S., C.E. Oakley, G. Chen, X. Han, B.R. Oakley, and X. Xiang. 2005b. Cytoplasmic dynein's mitotic spindle pole localization requires a functional anaphase-promoting complex, gamma-tubulin, and NUDF/LIS1 in Aspergillus nidulans. *Mol. Biol. Cell.* 16:3591–3605. https://doi.org/10.1091/mbc.e04-12-1071

Li, Y.Y., E. Yeh, T. Hays, and K. Bloom. 1993. Disruption of mitotic spindle orientation in a yeast dynein mutant. *Proc. Natl. Acad. Sci. USA.* 90:10096–10100. https://doi.org/10.1073/pnas.90.21.10096

Liang, Y., W. Yu, Y. Li, Z. Yang, X. Yan, Q. Huang, and X. Zhu. 2004. Nudel functions in membrane traffic mainly through association with Lis1 and cytoplasmic dynein. *J. Cell Biol.* 164:557–566. https://doi.org/10.1083/jcb.200308058

Liang, Y., W. Yu, Y. Li, L. Yu, Q. Zhang, F. Wang, Z. Yang, J. Du, Q. Huang, X. Yao, and X. Zhu. 2007. Nudel modulates kinetochore association and function of cytoplasmic dynein in M phase. *Mol. Biol. Cell.* 18:2656–2666. https://doi.org/10.1091/mbc.e06-04-0345

Liu, B., X. Xiang, and Y.R. Lee. 2003. The requirement of the LC8 dynein light chain for nuclear migration and septum positioning is temperature dependent in Aspergillus nidulans. *Mol. Microbiol.* 47:291–301. https://doi.org/10.1046/j.1365-2958.2003.03285.x

Lomakin, A.J., I. Semenova, I. Zaliapin, P. Kraikivski, E. Nadezhdina, B.M. Slepchenko, A. Akhmanova, and V. Rodionov. 2009. CLIP-170-dependent capture of membrane organelles by microtubules initiates minus-end directed transport. *Dev. Cell.* 17:323–333. https://doi.org/10.1016/j.devcel.2009.07.010

Ma, L., M.Y. Tsai, S. Wang, B. Lu, R. Chen, J.R. Yates III, X. Zhu, and Y. Zheng. 2009. Requirement for Nudel and dynein for assembly of the lamin B spindle matrix. *Nat. Cell Biol.* 11:247–256. https://doi.org/10.1038/ncb1832

Maday, S., A.E. Twelvetrees, A.J. Moughamian, and E.L. Holzbaur. 2014. Axonal transport: cargo-specific mechanisms of motility and regulation. *Neuron.* 84:292–309. https://doi.org/10.1016/j.neuron.2014.10.019

Marzo, M.G., J.M. Griswold, and S.M. Markus. 2019. Pac1/LIS1 promotes an uninhibited conformation of dynein that coordinates its localization and activity. *bioRxiv.* https://doi.org/10.1101/684290 (Preprint posted June 27, 2019)

McKenney, R.J., M. Vershinin, A. Kunwar, R.B. Vallee, and S.P. Gross. 2010. LIS1 and NudE induce a persistent dynein force-producing state. *Cell.* 141:304–314. https://doi.org/10.1016/j.cell.2010.02.035

McKenney, R.J., S.J. Weil, J. Scherer, and R.B. Vallee. 2011. Mutually exclusive cytoplasmic dynein regulation by NudE-Lis1 and dynactin. *J. Biol. Chem.* 286:39615–39622. https://doi.org/10.1074/jbc.M111.289017

McKenney, R.J., W. Huynh, M.E. Tanenbaum, G. Bhabha, and R.D. Vale. 2014. Activation of cytoplasmic dynein motility by dynactin-cargo adapter complexes. *Science.* 345:337–341. https://doi.org/10.1126/science.1254198

McKenney, R.J., W. Huynh, R.D. Vale, and M. Sirajuddin. 2016. Tyrosination of α-tubulin controls the initiation of processive dynein-dynactin motility. *EMBO J.* 35:1175–1185. https://doi.org/10.15252/embj.201593071

Minke, P.F., I.H. Lee, J.H. Tinsley, K.S. Bruno, and M. Plamann. 1999. Neurospora crassa ro-10 and ro-11 genes encode novel proteins required for nuclear distribution. *Mol. Microbiol.* 32:1065–1076. https://doi.org/10.1046/j.1365-2958.1999.01421.x

Moore, J.K., J. Li, and J.A. Cooper. 2008. Dynactin function in mitotic spindle positioning. *Traffic.* 9:510–527. https://doi.org/10.1111/j.1600-0854.2008.00710.x

Moughamian, A.J., G.E. Osborn, J.E. Lazarus, S. Maday, and E.L. Holzbaur. 2013. Ordered recruitment of dynactin to the microtubule plus-end is required for efficient initiation of retrograde axonal transport. *J. Neurosci.* 33:13190–13203. https://doi.org/10.1523/JNEUROSCI.0935-13.2013

Nicholas, M.P., F. Berger, L. Rao, S. Brenner, C. Cho, and A. Gennerich. 2015. Cytoplasmic dynein regulates its attachment to microtubules via nucleotide state-switched mechanosensing at multiple AAA domains. *Proc. Natl. Acad. Sci. USA.* 112:6371–6376. https://doi.org/10.1073/pnas.1417422112

Niethammer, M., D.S. Smith, R. Ayala, J. Peng, J. Ko, M.S. Lee, M. Morabito, and L.H. Tsai. 2000. NUDEL is a novel Cdk5 substrate that associates with LIS1 and cytoplasmic dynein. *Neuron.* 28:697–711. https://doi.org/10.1016/S0896-6273(00)00147-1

Nirschl, J.J., M.M. Magiera, J.E. Lazarus, C. Janke, and E.L. Holzbaur. 2016. α-Tubulin Tyrosination and CLIP-170 Phosphorylation Regulate the Initiation of Dynein-Driven Transport in Neurons. *Cell Reports.* 14:2637–2652. https://doi.org/10.1016/j.celrep.2016.02.046

Oakley, B.R., C.E. Oakley, Y. Yoon, and M.K. Jung. 1990. Gamma-tubulin is a component of the spindle pole body that is essential for microtubule function in Aspergillus nidulans. *Cell.* 61:1289–1301. https://doi.org/10.1016/0092-8674(90)90693-9

Olenick, M.A., and E.L.F. Holzbaur. 2019. Dynein activators and adaptors at a glance. *J. Cell Sci.* 132:jcs227132. https://doi.org/10.1242/jcs.227132

Olenick, M.A., M. Tokito, M. Boczkowska, R. Dominguez, and E.L. Holzbaur. 2016. Hook Adaptors Induce Unidirectional Processive Motility by Enhancing the Dynein-Dynactin Interaction. *J. Biol. Chem.* 291:18239–18251. https://doi.org/10.1074/jbc.M116.738211

Olenick, M.A., R. Dominguez, and E.L.F. Holzbaur. 2019. Dynein activator Hook1 is required for trafficking of BDNF-signaling endosomes in neurons. *J. Cell Biol.* 218:220–233. https://doi.org/10.1083/jcb.201805016

Omer, S., S.R. Greenberg, and W.L. Lee. 2018. Cortical dynein pulling mechanism is regulated by differentially targeted attachment molecule Num1. *eLife.* 7:e36745. https://doi.org/10.7554/eLife.36745

Ori-McKenney, K.M., J. Xu, S.P. Gross, and R.B. Vallee. 2010. A cytoplasmic dynein tail mutation impairs motor processivity. *Nat. Cell Biol.* 12:1228–1234. https://doi.org/10.1038/ncb2127

Otamendi, A., E. Perez-de-Nanclares-Arregi, E. Oiartzabal-Arano, M.S. Cortese, E.A. Espeso, and O. Etxebeste. 2019. Developmental regulators FlbE/D orchestrate the polarity site-to-nucleus dynamics of the fungal bZIP transcription factor FlbB. *Cell. Mol. Life Sci.* https://doi.org/10.1007/s00018-019-03121-5

Pandey, J.P., and D.S. Smith. 2011. A Cdk5-dependent switch regulates Lis1/Ndel1/dynein-driven organelle transport in adult axons. *J. Neurosci.* 31:17207–17219. https://doi.org/10.1523/JNEUROSCI.4108-11.2011

Pantazopoulou, A., and M.A. Peñalva. 2009. Organization and dynamics of the Aspergillus nidulans Golgi during apical extension and mitosis. *Mol. Biol. Cell.* 20:4335–4347. https://doi.org/10.1091/mbc.e09-03-0254

Pedersen, L.B., P. Rompolas, S.T. Christensen, J.L. Rosenbaum, and S.M. King. 2007. The lissencephaly protein Lis1 is present in motile mammalian cilia and requires outer arm dynein for targeting to Chlamydomonas flagella. *J. Cell Sci.* 120:858–867. https://doi.org/10.1242/jcs.03374

Peñalva, M.A., J. Zhang, X. Xiang, and A. Pantazopoulou. 2017. Transport of fungal RAB11 secretory vesicles involves myosin-5, dynein/dynactin/

p25, and kinesin-1 and is independent of kinesin-3. *Mol. Biol. Cell.* 28: 947–961. https://doi.org/10.1091/mbc.e16-08-0566

Plamann, M., P.F. Minke, J.H. Tinsley, and K.S. Bruno. 1994. Cytoplasmic dynein and actin-related protein Arp1 are required for normal nuclear distribution in filamentous fungi. *J. Cell Biol.* 127:139–149. https://doi.org/10.1083/jcb.127.1.139

Pohlmann, T., S. Baumann, C. Haag, M. Albrecht, and M. Feldbrügge. 2015. A FYVE zinc finger domain protein specifically links mRNA transport to endosome trafficking. *eLife.* 4:e06041. https://doi.org/10.7554/eLife.06041

Qiu, R., J. Zhang, and X. Xiang. 2013. Identification of a novel site in the tail of dynein heavy chain important for dynein function in vivo. *J. Biol. Chem.* 288:2271–2280. https://doi.org/10.1074/jbc.M112.412403

Qiu, R., J. Zhang, and X. Xiang. 2018. p25 of the dynactin complex plays a dual role in cargo binding and dynactin regulation. *J. Biol. Chem.* 293: 15606–15619. https://doi.org/10.1074/jbc.RA118.004000

Raaijmakers, J.A., M.E. Tanenbaum, and R.H. Medema. 2013. Systematic dissection of dynein regulators in mitosis. *J. Cell Biol.* 201:201–215. https://doi.org/10.1083/jcb.201208098

Rao, L., E.M. Romes, M.P. Nicholas, S. Brenner, A. Tripathy, A. Gennerich, and K.C. Slep. 2013. The yeast dynein Dyn2-Pac11 complex is a dynein dimerization/processivity factor: structural and single-molecule characterization. *Mol. Biol. Cell.* 24:2362–2377. https://doi.org/10.1091/mbc.e13-03-0166

Reck-Peterson, S.L., W.B. Redwine, R.D. Vale, and A.P. Carter. 2018. The cytoplasmic dynein transport machinery and its many cargoes. *Nat. Rev. Mol. Cell Biol.* 19:382–398. https://doi.org/10.1038/s41580-018-0004-3

Reddy, B.J., M. Mattson, C.L. Wynne, O. Vadpey, A. Durra, D. Chapman, R.B. Vallee, and S.P. Gross. 2016. Load-induced enhancement of Dynein force production by LIS1-NudE in vivo and in vitro. *Nat. Commun.* 7: 12259. https://doi.org/10.1038/ncomms12259

Reiner, O., R. Carrozzo, Y. Shen, M. Wehnert, F. Faustinella, W.B. Dobyns, C.T. Caskey, and D.H. Ledbetter. 1993. Isolation of a Miller-Dieker lissencephaly gene containing G protein beta-subunit-like repeats. *Nature.* 364:717–721. https://doi.org/10.1038/364717a0

Requena, N., C. Alberti-Segui, E. Winzenburg, C. Horn, M. Schliwa, P. Philippsen, R. Liese, and R. Fischer. 2001. Genetic evidence for a microtubule-destabilizing effect of conventional kinesin and analysis of its consequences for the control of nuclear distribution in Aspergillus nidulans. *Mol. Microbiol.* 42:121–132. https://doi.org/10.1046/j.1365-2958.2001.02609.x

Roberts, A.J. 2018. Emerging mechanisms of dynein transport in the cytoplasm versus the cilium. *Biochem. Soc. Trans.* 46:967–982. https://doi.org/10.1042/BST20170568

Roberts, A.J., B.S. Goodman, and S.L. Reck-Peterson. 2014. Reconstitution of dynein transport to the microtubule plus end by kinesin. *eLife.* 3:e02641. https://doi.org/10.7554/eLife.02641

Rompolas, P., R.S. Patel-King, and S.M. King. 2012. Association of Lis1 with outer arm dynein is modulated in response to alterations in flagellar motility. *Mol. Biol. Cell.* 23:3554–3565. https://doi.org/10.1091/mbc.e12-04-0287

Salogiannis, J., M.J. Egan, and S.L. Reck-Peterson. 2016. Peroxisomes move by hitchhiking on early endosomes using the novel linker protein PxdA. *J. Cell Biol.* 212:289–296. https://doi.org/10.1083/jcb.201512020

Sasaki, S., A. Shionoya, M. Ishida, M.J. Gambello, J. Yingling, A. Wynshaw-Boris, and S. Hirotsune. 2000. A LIS1/NUDEL/cytoplasmic dynein heavy chain complex in the developing and adult nervous system. *Neuron.* 28:681–696. https://doi.org/10.1016/S0896-6273(00)00146-X

Schlager, M.A., H.T. Hoang, L. Urnavicius, S.L. Bullock, and A.P. Carter. 2014. In vitro reconstitution of a highly processive recombinant human dynein complex. *EMBO J.* 33:1855–1868. https://doi.org/10.15252/embj.201488792

Schroeder, C.M., and R.D. Vale. 2016. Assembly and activation of dynein-dynactin by the cargo adaptor protein Hook3. *J. Cell Biol.* 214:309–318. https://doi.org/10.1083/jcb.201604002

Schroer, T.A. 2004. Dynactin. *Annu. Rev. Cell Dev. Biol.* 20:759–779. https://doi.org/10.1146/annurev.cellbio.20.012103.094623

Schuster, M., R. Lipowsky, M.A. Assmann, P. Lenz, and G. Steinberg. 2011. Transient binding of dynein controls bidirectional long-range motility of early endosomes. *Proc. Natl. Acad. Sci. USA.* 108:3618–3623. https://doi.org/10.1073/pnas.1015839108

Seidel, C., S.D. Moreno-Velásquez, M. Riquelme, and R. Fischer. 2013. Neurospora crassa NKIN2, a kinesin-3 motor, transports early endosomes and is required for polarized growth. *Eukaryot. Cell.* 12:1020–1032. https://doi.org/10.1128/EC.00081-13

Sheeman, B., P. Carvalho, I. Sagot, J. Geiser, D. Kho, M.A. Hoyt, and D. Pellman. 2003. Determinants of S. cerevisiae dynein localization and activation: implications for the mechanism of spindle positioning. *Curr. Biol.* 13:364–372. https://doi.org/10.1016/S0960-9822(03)00013-7

Shen, K.F., and S.A. Osmani. 2013. Regulation of mitosis by the NIMA kinase involves TINA and its newly discovered partner, An-WDR8, at spindle pole bodies. *Mol. Biol. Cell.* 24:3842–3856. https://doi.org/10.1091/mbc.e13-07-0422

Shu, T., R. Ayala, M.D. Nguyen, Z. Xie, J.G. Gleeson, and L.H. Tsai. 2004. Ndel1 operates in a common pathway with LIS1 and cytoplasmic dynein to regulate cortical neuronal positioning. *Neuron.* 44:263–277. https://doi.org/10.1016/j.neuron.2004.09.030

Simões, P.A., R. Celestino, A.X. Carvalho, and R. Gassmann. 2018. NudE regulates dynein at kinetochores but is dispensable for other dynein functions in the C. elegans early embryo. *J. Cell Sci.* 131:jcs212159. https://doi.org/10.1242/jcs.212159

Splinter, D., D.S. Razafsky, M.A. Schlager, A. Serra-Marques, I. Grigoriev, J. Demmers, N. Keijzer, K. Jiang, I. Poser, A.A. Hyman, et al. 2012. BICD2, dynactin, and LIS1 cooperate in regulating dynein recruitment to cellular structures. *Mol. Biol. Cell.* 23:4226–4241. https://doi.org/10.1091/mbc.e12-03-0210

Stehman, S.A., Y. Chen, R.J. McKenney, and R.B. Vallee. 2007. NudE and NudEL are required for mitotic progression and are involved in dynein recruitment to kinetochores. *J. Cell Biol.* 178:583–594. https://doi.org/10.1083/jcb.200610112

Steinberg, G. 2015. Kinesin-3 in the basidiomycete Ustilago maydis transports organelles along the entire microtubule array. *Fungal Genet. Biol.* 74: 59–61. https://doi.org/10.1016/j.fgb.2014.10.010

Tas, R.P., A. Chazeau, B.M.C. Cloin, M.L.A. Lambers, C.C. Hoogenraad, and L.C. Kapitein. 2017. Differentiation between Oppositely Oriented Microtubules Controls Polarized Neuronal Transport. *Neuron.* 96: 1264–1271.e5. https://doi.org/10.1016/j.neuron.2017.11.018

Torisawa, T., A. Nakayama, K. Furuta, M. Yamada, S. Hirotsune, and Y.Y. Toyoshima. 2011. Functional dissection of LIS1 and NDEL1 towards understanding the molecular mechanisms of cytoplasmic dynein regulation. *J. Biol. Chem.* 286:1959–1965. https://doi.org/10.1074/jbc.M110.169847

Torisawa, T., M. Ichikawa, A. Furuta, K. Saito, K. Oiwa, H. Kojima, Y.Y. Toyoshima, and K. Furuta. 2014. Autoinhibition and cooperative activation mechanisms of cytoplasmic dynein. *Nat. Cell Biol.* 16:1118–1124. https://doi.org/10.1038/ncb3048

Toropova, K., S. Zou, A.J. Roberts, W.B. Redwine, B.S. Goodman, S.L. Reck-Peterson, and A.E. Leschziner. 2014. Lis1 regulates dynein by sterically blocking its mechanochemical cycle. *eLife.* 3:e03372. https://doi.org/10.7554/eLife.03372

Toropova, K., M. Mladenov, and A.J. Roberts. 2017. Intraflagellar transport dynein is autoinhibited by trapping of its mechanical and track-binding elements. *Nat. Struct. Mol. Biol.* 24:461–468. https://doi.org/10.1038/nsmb.3391

Twelvetrees, A.E., S. Pernigo, A. Sanger, P. Guedes-Dias, G. Schiavo, R.A. Steiner, M.P. Dodding, and E.L. Holzbaur. 2016. The Dynamic Localization of Cytoplasmic Dynein in Neurons Is Driven by Kinesin-1. *Neuron.* 90:1000–1015. https://doi.org/10.1016/j.neuron.2016.04.046

Urnavicius, L., C.K. Lau, M.M. Elshenawy, E. Morales-Rios, C. Motz, A. Yildiz, and A.P. Carter. 2018. Cryo-EM shows how dynactin recruits two dyneins for faster movement. *Nature.* 554:202–206. https://doi.org/10.1038/nature25462

Vallee, R.B., R.J. McKenney, and K.M. Ori-McKenney. 2012. Multiple modes of cytoplasmic dynein regulation. *Nat. Cell Biol.* 14:224–230. https://doi.org/10.1038/ncb2420

Vaughan, K.T., and R.B. Vallee. 1995. Cytoplasmic dynein binds dynactin through a direct interaction between the intermediate chains and p150Glued. *J. Cell Biol.* 131:1507–1516. https://doi.org/10.1083/jcb.131.6.1507

Vaughan, P.S., P. Miura, M. Henderson, B. Byrne, and K.T. Vaughan. 2002. A role for regulated binding of p150(Glued) to microtubule plus ends in organelle transport. *J. Cell Biol.* 158:305–319. https://doi.org/10.1083/jcb.200201029

Walenta, J.H., A.J. Didier, X. Liu, and H. Krämer. 2001. The Golgi-associated hook3 protein is a member of a novel family of microtubule-binding proteins. *J. Cell Biol.* 152:923–934. https://doi.org/10.1083/jcb.152.5.923

Wang, S., and Y. Zheng. 2011. Identification of a novel dynein binding domain in nudel essential for spindle pole organization in Xenopus egg extract. *J. Biol. Chem.* 286:587–593. https://doi.org/10.1074/jbc.M110.181578

Wang, S., S.A. Ketcham, A. Schön, B. Goodman, Y. Wang, J. Yates III, E. Freire, T.A. Schroer, and Y. Zheng. 2013. Nudel/NudE and Lis1 promote dynein

and dynactin interaction in the context of spindle morphogenesis. *Mol. Biol. Cell.* 24:3522–3533. https://doi.org/10.1091/mbc.e13-05-0283

Wedlich-Söldner, R., A. Straube, M.W. Friedrich, and G. Steinberg. 2002. A balance of KIF1A-like kinesin and dynein organizes early endosomes in the fungus Ustilago maydis. *EMBO J.* 21:2946–2957. https://doi.org/10.1093/emboj/cdf296

Willins, D.A., B. Liu, X. Xiang, and N.R. Morris. 1997. Mutations in the heavy chain of cytoplasmic dynein suppress the nudF nuclear migration mutation of Aspergillus nidulans. *Mol. Gen. Genet.* 255:194–200. https://doi.org/10.1007/s004380050489

Xiang, X. 2018. Nuclear movement in fungi. *Semin. Cell Dev. Biol.* 82:3–16. https://doi.org/10.1016/j.semcdb.2017.10.024

Xiang, X., S.M. Beckwith, and N.R. Morris. 1994. Cytoplasmic dynein is involved in nuclear migration in Aspergillus nidulans. *Proc. Natl. Acad. Sci. USA.* 91:2100–2104. https://doi.org/10.1073/pnas.91.6.2100

Xiang, X., A.H. Osmani, S.A. Osmani, M. Xin, and N.R. Morris. 1995a. NudF, a nuclear migration gene in Aspergillus nidulans, is similar to the human LIS-1 gene required for neuronal migration. *Mol. Biol. Cell.* 6:297–310. https://doi.org/10.1091/mbc.6.3.297

Xiang, X., C. Roghi, and N.R. Morris. 1995b. Characterization and localization of the cytoplasmic dynein heavy chain in Aspergillus nidulans. *Proc. Natl. Acad. Sci. USA.* 92:9890–9894. https://doi.org/10.1073/pnas.92.21.9890

Xiong, Y., and B.R. Oakley. 2009. In vivo analysis of the functions of gamma-tubulin-complex proteins. *J. Cell Sci.* 122:4218–4227. https://doi.org/10.1242/jcs.059196

Xu, L., M.E. Sowa, J. Chen, X. Li, S.P. Gygi, and J.W. Harper. 2008. An FTS/Hook/p107(FHIP) complex interacts with and promotes endosomal clustering by the homotypic vacuolar protein sorting complex. *Mol. Biol. Cell.* 19:5059–5071. https://doi.org/10.1091/mbc.e08-05-0473

Yamada, M., S. Toba, Y. Yoshida, K. Haratani, D. Mori, Y. Yano, Y. Mimori-Kiyosue, T. Nakamura, K. Itoh, S. Fushiki, et al. 2008. LIS1 and NDEL1 coordinate the plus-end-directed transport of cytoplasmic dynein. *EMBO J.* 27:2471–2483. https://doi.org/10.1038/emboj.2008.182

Yao, X., J. Zhang, H. Zhou, E. Wang, and X. Xiang. 2012. In vivo roles of the basic domain of dynactin p150 in microtubule plus-end tracking and dynein function. *Traffic.* 13:375–387. https://doi.org/10.1111/j.1600-0854.2011.01312.x

Yao, X., X. Wang, and X. Xiang. 2014. FHIP and FTS proteins are critical for dynein-mediated transport of early endosomes in Aspergillus. *Mol. Biol. Cell.* 25:2181–2189. https://doi.org/10.1091/mbc.e14-04-0873

Yeh, T.Y., N.J. Quintyne, B.R. Scipioni, D.M. Eckley, and T.A. Schroer. 2012. Dynactin's pointed-end complex is a cargo-targeting module. *Mol. Biol. Cell.* 23:3827–3837. https://doi.org/10.1091/mbc.e12-07-0496

Zekert, N., and R. Fischer. 2009. The Aspergillus nidulans kinesin-3 UncA motor moves vesicles along a subpopulation of microtubules. *Mol. Biol. Cell.* 20:673–684. https://doi.org/10.1091/mbc.e08-07-0685

Zekert, N., D. Veith, and R. Fischer. 2010. Interaction of the Aspergillus nidulans microtubule-organizing center (MTOC) component ApsB with gamma-tubulin and evidence for a role of a subclass of peroxisomes in the formation of septal MTOCs. *Eukaryot. Cell.* 9:795–805. https://doi.org/10.1128/EC.00058-10

Zeng, C.J., H.R. Kim, I. Vargas Arispuro, J.M. Kim, A.C. Huang, and B. Liu. 2014. Microtubule plus end-tracking proteins play critical roles in directional growth of hyphae by regulating the dynamics of cytoplasmic microtubules in Aspergillus nidulans. *Mol. Microbiol.* 94:506–521. https://doi.org/10.1111/mmi.12792

Zhang, J., S. Li, R. Fischer, and X. Xiang. 2003. Accumulation of cytoplasmic dynein and dynactin at microtubule plus ends in Aspergillus nidulans is kinesin dependent. *Mol. Biol. Cell.* 14:1479–1488. https://doi.org/10.1091/mbc.e02-08-0516

Zhang, J., L. Wang, L. Zhuang, L. Huo, S. Musa, S. Li, and X. Xiang. 2008. Arp11 affects dynein-dynactin interaction and is essential for dynein function in Aspergillus nidulans. *Traffic.* 9:1073–1087. https://doi.org/10.1111/j.1600-0854.2008.00748.x

Zhang, J., L. Zhuang, Y. Lee, J.F. Abenza, M.A. Peñalva, and X. Xiang. 2010. The microtubule plus-end localization of Aspergillus dynein is important for dynein-early-endosome interaction but not for dynein ATPase activation. *J. Cell Sci.* 123:3596–3604. https://doi.org/10.1242/jcs.075259

Zhang, J., X. Yao, L. Fischer, J.F. Abenza, M.A. Peñalva, and X. Xiang. 2011. The p25 subunit of the dynactin complex is required for dynein-early endosome interaction. *J. Cell Biol.* 193:1245–1255. https://doi.org/10.1083/jcb.201011022

Zhang, J., R. Qiu, H.N. Arst Jr., M.A. Peñalva, and X. Xiang. 2014. HookA is a novel dynein-early endosome linker critical for cargo movement in vivo. *J. Cell Biol.* 204:1009–1026. https://doi.org/10.1083/jcb.201308009

Zhang, J., R. Qiu, and X. Xiang. 2018. The actin capping protein in Aspergillus nidulans enhances dynein function without significantly affecting Arp1 filament assembly. *Sci. Rep.* 8:11419. https://doi.org/10.1038/s41598-018-29818-4

Zhang, K., H.E. Foster, A. Rondelet, S.E. Lacey, N. Bahi-Buisson, A.W. Bird, and A.P. Carter. 2017a. Cryo-EM Reveals How Human Cytoplasmic Dynein Is Auto-inhibited and Activated. *Cell.* 169:1303–1314.e18. https://doi.org/10.1016/j.cell.2017.05.025

Zhang, Q., F. Wang, J. Cao, Y. Shen, Q. Huang, L. Bao, and X. Zhu. 2009. Nudel promotes axonal lysosome clearance and endo-lysosome formation via dynein-mediated transport. *Traffic.* 10:1337–1349. https://doi.org/10.1111/j.1600-0854.2009.00945.x

Zhang, Y., X. Gao, R. Manck, M. Schmid, A.H. Osmani, S.A. Osmani, N. Takeshita, and R. Fischer. 2017b. Microtubule-organizing centers of Aspergillus nidulans are anchored at septa by a disordered protein. *Mol. Microbiol.* 106:285–303. https://doi.org/10.1111/mmi.13763

Zyłkiewicz, E., M. Kijańska, W.C. Choi, U. Derewenda, Z.S. Derewenda, and P.T. Stukenberg. 2011. The N-terminal coiled-coil of Ndel1 is a regulated scaffold that recruits LIS1 to dynein. *J. Cell Biol.* 192:433–445. https://doi.org/10.1083/jcb.201011142